INVESTIGATION OF THROUGH-THICKNESS PROPERTIES OF ROLLED WIDE FLANGE SHAPES

by

SHIH-HSIUNG WANG, B.S.

THESIS

Presented to the Faculty of the Graduate School
of the University of Texas at Austin
in Partial Fulfillment of
the Requirements
for the Degree of

MASTER OF SCIENCE IN ENGINEERING

THE UNIVERSITY OF TEXAS AT AUSTIN

AUGUST,1997

INVESTIGATION OF THROUGH-THICKNESS PROPERTIES OF ROLLED WIDE FLANGE SHAPES

APPROVED

Dr. Michael D. Engelhardt

Dr. Karl H. Frank

To my parents.

ACKNOWLEDGEMENTS

First of all I would like to thank Dr. Michael D. Engelhardt, not only for his invaluable advice, guidance, assistance and patience as my thesis advisor, but also for his friendship and support during my days in Austin. It was a great honor to be his student. I also wish to thank Dr. Karl H. Frank for serving as a second reader, for his valuable recommendations and suggestions.

I would also like to thank the staff of the Ferguson Lab, in the office and on the lab floor, they have always been there to help the students when necessary.

To the graduate students in the Ferguson Lab, for all of their advice and friendship during the time I worked in the Lab. It's been my pleasure to work with these outstanding students.

To the officers of the Chinese Student Association and Chao Wen Fu for all of their efforts, encouragement, sacrifice, and most of all, their everlasting love.

Finally, I would like to thank my family for their unending, selfless support throughout my life and education

Shih-Hsiung Wang

May 26,1997 Austin, Texas

ABSTRACT

INVESTIGATION OF THROUGH-THICKNESS PROPERTIES OF ROLLED WIDE FLANGE SHAPES

by

Shih-Hsiung Wang, M.S.E

The University of Texas at Austin, 1997

Supervising Professor: Michael D. Engelhardt

This thesis examines methods for measuring through-thickness tensile properties of a sample of steel taken from the flange of a W14x426 rolled wide flange shape made of A572 Gr. 50 Steel. This study was motivated by the widespread failure of welded moment connections in the Northridge Earthquake. These failures have raised concerns about possible deficient through-thickness properties of column flanges. Through-thickness tension tests are not routinely performed on rolled shapes in current construction practice, and test methods are not well developed or documented.

The primary objective of this thesis was to compare two different methods of preparing through-thickness tension coupons, and to determine if reliable measurements of strength and ductility are possible with these coupon types. One coupon type was a sub-length coupon, machined directly from the 3 inch thick column flange, and tested without the use of welded prolongations. The second coupon type was prepared by welding high strength prolongations onto the column flange material. For each coupon type, samples were prepared and tested in both the rolling direction and through-thickness direction to provide a more

thorough evaluation of the influence of coupon design on the measured mechanical properties.

The test results indicate that reliable and repeatable measurements of ultimate stress and reduction of area were possible with both coupon types. Measurements of yield stress, however, were not consistent between the two types of coupons. The welded coupons in the through-thickness direction gave significantly higher yield stress measurements than the sub-length coupons.

For the sample of steel tested in this research program, the ultimate stress in the through-thickness and rolling directions were nearly identical. The ductility, as measured by reduction of area, was significantly lower in the through-thickness direction as compared with the rolling direction.

TABLE OF CONTENTS

LIST OF TABLES

LIST OF FIGURES

CHAPTER 1

INTRODUCTION

1.1 Background

Tensile tests are routinely conducted on structural steel that is to be used in buildings and other types of structures. The results of tensile tests provide the material properties that are needed in design. They are also conducted in order to ensure quality and conformance to material specifications. Tensile properties are often measured during the development of new materials and processes, so that different materials and processes can be compared. Finally, tensile properties are often used to predict the behavior of a material under various forms of loading other than uniaxial tension.

Tensile tests provide several material properties which are of interest in the design of steel structures. Strength is often a primary concern. The strength of interest may be measured in terms of either the stress necessary to cause appreciable plastic deformation (yield stress, F_y), or the maximum stress that the material can withstand (ultimate tensile strength, F_u). These measures of strength are used, with appropriate safety factors, in the process of engineering design. Also of interest is the material's ductility: a measure of how much it can be plastically deformed before it fractures. In a tensile test of steel, ductility is commonly measured as being the percent elongation or percent reduction in area of the tensile coupon at fracture. Ductility is rarely directly incorporated into the design process. Rather, ductility is relied upon implicitly in the design of steel

structures so as to provide for the redistribution of stresses and forces within the structure. For example, when analyzed elastically, typical bolted and welded connections in steel frames normally show large stress concentrations. The ductility of steel allows for the redistribution of these locally high stresses, which in turn allows larger forces on the connection prior to fracture. The internal redistribution of stresses in a ductile material also simplifies design by eliminating the need to calculate the stress concentration factors in most design computations for steel buildings. On the other hand, quantifying the amount of material ductility needed for a particular member or connection in a steel structure is often a difficult matter.

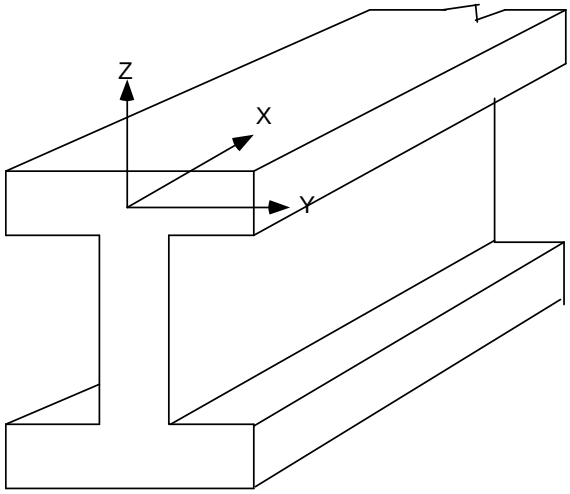

Fig 1.1 A Rolled W-Shape with a Cartesian Coordinate System

For rolled steel shapes and plates, tensile coupons are normally taken along the rolling direction. For example, Fig. 1.1 shows a rolled W-Shape with a

Cartesian coordinate system that is superimposed on the flange. The X direction coincides with the rolling direction. A tensile coupon that is intended to measure the mechanical properties of the flange material would normally be oriented in the X direction. The Y direction is transverse to the rolling direction in the plane of the flange. Finally, the Z direction, which is also normal to the rolling direction, coincides with the through-thickness direction of the flange.

In typical design practice for buildings, steel is treated as a homogeneous isotropic material. Thus, material properties that are measured in the rolling direction are normally used in design calculations regardless of the direction of the applied stress in the actual member. However, it has long been recognized that commercially available rolled plates and shapes can exhibit anisotropic material properties. In particular, the strength and ductility in the through-thickness direction can be substantially different, and is often less than the strength and ductility in the rolling direction. Reduced strength and ductility in the through-thickness direction has usually been attributed to the presence of non-metallic inclusions that assume a flat shape during the rolling process. These flat elongated inclusions are oriented parallel to the surface of the plate and form pre-existing planes of weakness for tensile loading in the through-thickness direction. Consequently, fracture can occur in the through-thickness direction at levels of stress and ductility which are substantially less than that of the rolling direction. The fracture of steel in the through-thickness direction can occur along these pre-existing planes of weakness, resulting in a phenomena known as lamellar tearing. Although it appears such problems have been infrequent, problems with lamellar tearing have been observed in the past in structural steel buildings[1]. Typically, lamellar tearing problems have occurred in welded joints where weld shrinkage provided the source of through-thickness tensile stress and induced lamellar

tearing. These problems have often been addressed by an improved detailing of the welded joint combined with improved through-thickness properties. Because lamellar tearing apparently has not been a widespread problem in past practice, through-thickness tensile testing of structural steel shapes and plates has not been a significant concern in the building construction industry.

Renewed concern about the through-thickness properties of rolled structural steel shapes has been generated as a result of the 1994 Northridge Earthquake. Widespread failure of welded beam-to-column moment connections was observed in this earthquake. One of the connection failure modes observed was a "divot" type fracture in the column flange at the beam flange groove weld. In this failure mode, a "divot" of column flange material was pulled from the column flange, with a portion of the fracture surface running approximately parallel to the face of the column. These fractures raised concerns about possible deficiencies in the through-thickness properties of column flanges[2]. Similar concerns were raised as a result of an apparent through-thickness failure of a column flange in a laboratory test of a steel moment connection[3]. Subsequent studies indicated that both the field and laboratory column fractures initiated at the groove weld, and that deficient through-thickness material properties were likely not a primary cause of the failures[4,5]. Nevertheless, these failures highlighted the lack of data available on actual through-thickness properties of rolled W-shape flanges, and significant concerns remain regarding these properties. Concerns raised by the Northridge Earthquake in regard to through-thickness properties of rolled shapes provided the motivation for this thesis.

1.2 Summary of Previous Research on Methods for Through Thickness

Testing

ASTM has recognized the need to address the subject of through-thickness tension testing. A task-force was formed in order to write a specification for testing procedures for the determination of through-thickness reduction of area values in plates over 1 in (25.4 mm) thick. The principle purpose of the testing was to provide a method for evaluating the susceptibility of a steel plate to lamellar tearing. This work resulted in the ASTM standard known as "Specification for Through-Thickness Tension Testing of Steel Plate for Special Applications" (A770), which was approved by the society on 28 March 1980. A copy of ASTM A770 is included in Appendix A of this report. In the process of writing ASTM A770, it became clear to those involved that through-thickness tension testing had a set of characteristics quite different from those normally associated with in-plane testing (longitudinal or transverse to the rolling direction). Some of the factors considered were the effects of specimen design, preparation, location in the plate, and the inherent variability of test results.

Holt [6] conducted a study in order to evaluate the effect of gage length on the tensile-strength and reduction-in-area values obtained for stub and tab specimens that are used to measure the through-thickness tension properties of plate steels. In stub specimens, the length of the reduced section of the standard specimen is shortened, while the other dimensions remain unchanged, so that the overall length of the specimen doesn't exceed the thickness of the plate. While in tab specimens, high strength prolongations (tabs) are welded to the plate surfaces so as to obtain a sufficient length for a standard-size specimen. Three steel plate materials with a wide strength range were used in his investigation. Holt used either 0.5 or 0.9 in (12.7 or 22.8 mm) diameter specimens that were oriented in

the rolling direction, not in the through-thickness direction. This orientation was chosen so as to reduce the influence of the data scatter that is inherent in through-thickness direction testing. Holt concluded that a significant decrease in the reduction in area and a significant increase in the tensile strength of both types of specimens occurred as the thickness of the insert or the length of the reduced section was decreased to less than two times the diameter of the specimens. These trends were attributed to constraint in the plastic flow caused by the higher strength of the weld area of the tab specimens, or by the shoulders of the stub specimens.

Reed et al [7] compared miniature bottom head specimens (MBH) machined entirely from the plate versus stud-welded specimens (SW) with stud-welded prolongations for gripping in the test machine. The authors concluded that MBH and SW specimens give comparable results for plates of 1 in (25 mm) and heavier. For lighter gage plates, however, the stress state in the SW specimen yields low ductility values, most likely because of the low effective gage length /diameter ratios. The authors noted that this ratio became important only for those values less than 2.5, which is the minimum value allowed in ASTM A 770. The MBH can be used to determine the distribution of properties through the thickness of a plate and may be less costly than the SW in terms of manpower, materials, and equipment. The versatility of the MBH, along with its constancy of geometry and cost effectiveness, makes it the more desirable specimen for testing short transverse properties.

Ludwigson addressed through-thickness testing in several papers. In the first [8], he reviews an analysis of a standard-deviation study that was made using through-thickness reduction-of-area measurements in six tests taken from each of

108 plate materials. These values were obtained by testing 0.505-in (12.83-mm)-diameter specimens prepared from stud-welded assemblies. An average standard deviation of 5.1 percentage points was observed, a value much larger than that seen in its planar-direction counterparts. Regression analysis indicated that the standard deviation increased as the plate thickness increased and decreased as the mean through-thickness reduction-of-area (TTRA) value moved in either direction from 38 percent.

In his second paper[9], Ludwigson evaluated the influence of coupon thickness on tensile properties that were measured with through-thickness specimens prepared from stud-welded assemblies. Ludwigson recommends using a minimum effective gage length that is equal to the coupon diameter. Neither the prolongation nor the distance affected by the heat from welding the prolongation is included in the effective gage length.

Domis [10] describes a procedure for using stud-welded prolongations on plates for the preparation of through-thickness test specimens. The experimental results indicate that as long as the strength of the stud was greater than that of the test plate, the strength level of the stud had no apparent effect on the through-thickness tension test result.

Jesseman and Murphy [11] evaluated the effect of tension specimen design, specimen-to-specimen variability, the reproducibility of the final area measurement, and the effect of material factors such as material strength level, steel microstructure and sample location. They concluded that more than two tests per plate are necessary for a reasonable evaluation of the through-thickness reduction-in-area properties.

Ludwigson[12] also made an attempt to demonstrate an association between microstructure and inclusion levels in plate and their through-thickness ductility. He concluded that inclusions are the principle factor that leads to restricting through-thickness ductility, but that high strength or low toughness may also cause reduced through-thickness reduction-of-area values.

Past research indicates that the results of a through-thickness tension test can be significantly affected by the dimensions and method of preparation that are used for the coupon. Such past research appears to have been conducted on plate material, using grades of steel not commonly used in building construction. Little work appears to have been done on rolled shapes made of ASTM A36 or ASTM A572 Grade 50 steels, which are commonly used in constructing structural steel buildings.

1.3 Objectives

In this thesis, through-thickness tension tests are conducted on the flange of a rolled W-shape that is made of ASTM A572 Grade 50 steel. The objectives of these tests are to assess two different methods for preparing the through-thickness coupons, and to determine if the coupon preparation method substantially affects the test results. The two methods of coupon preparation are:

a) a coupon machined directly from the flange, and
b) a coupon prepared using welded prolongations

In order to provide a direct comparison between the rolling direction and through-thickness properties for similar types of coupons, coupons were also prepared and tested along the rolling direction of the flange. For both the rolling direction and the through thickness direction, a series of coupons were taken across the width of the flange so as to assess the variations in mechanical properties across the flange.

Overall, this project is only intended to be a brief pilot-study that examines some key issues involved in through thickness testing of W-Shape flanges and is not intended to be an exhaustive investigation of through thickness tensile testing. Rather, the results of this study are intended to provide information on areas where additional research is needed on through-thickness tensile testing of rolled steel shapes.

1.4 Overview of Thesis

This thesis is organized into five chapters. Chapter 1 provides an introduction and overview of this project. Chapter 2 discusses the specimen design and establishes the specimen preparation procedure. Chapter 3 covers the test setup, and test procedure. Chapter 4 presents the test results and discussion and will include a comparison of the data gathered from the testing of all of the different types of tensile coupons. Finally, a brief summary of the results, some conclusions, and recommendations for future research are given in Chapter 5.

CHAPTER 2

TENSILE SPECIMEN DESIGN

2.1 Introduction

Fig 2.1. shows a typical tension specimen with a reduced section and enlarged shoulders. The specimen can be either a flat plate, or a machined circular coupon. In either case, it has enlarged ends or shoulders for gripping. The most important part of the specimen is the reduced section. The cross-sectional area of this section is reduced relative to that of the remainder of the specimen so that deformation and failure will be localized in this region. The gage length is the region over which measurements are made and is centered within the reduced section. The distance between the ends of the gage length and the shoulders should be at least as large as the diameter of the reduced section and the total length of the reduced section should be at least four times that of the diameter. Otherwise, the stress state will be more complex than in simple tension. [13]

Fig 2.1 Typical Tension Specimen

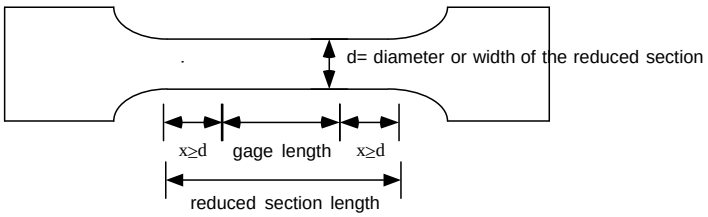

For testing in the rolling direction, dimensions for tension coupons are specified by ASTM A370 “Standard Methods and Definitions for Mechanical Testing of Steel Products”. Through-thickness (also known as short-transverse, or "Z" direction) tension testing has inherent difficulties that are quite separate from the more familiar in-plane testing procedures. Much of the work included in this Chapter is concerned with the design and the preparation of test specimens which will provide meaningful and repeatable results in the thorough-thickness direction.

There are several methods presently being used to measure through-thickness tensile properties of steel plates. These methods can be divided into two categories: specimens machined directly from the plate, and specimens with welded prolongations.

2.2 Specimen Design

To most accurately test the tensile properties in both the rolling direction and the through-thickness direction, the type of specimen must be properly considered. The ASTM A370 standard 0.5-in (12.7-mm)-diameter tension test specimen can be obtained in the rolling direction for plates having a length of about 4.5-in (114-mm) or greater, and in the Z-direction for plates having a thickness of about 4.5-in (114-mm) or greater. There are several ways to test thinner plates, such as:

(1). Use small-size specimens with dimensions that are proportional to those of the standard specimen.

Drawbacks:

a. The cross-section area may become so small that it may not be representative of the bulk material.

b. The material near the plate surfaces are not included in the gage length. The test results will therefore not be representative of the plate thickness in it's entirety.

c. Many commercial testing laboratories may not be equipped to machine or test such specimens.

Advantages:

The small-size specimens are ideally suited for light gage plates and have the ability to test specific regions of a plate, such as the surface, quarterline or centerline, through positioning of the specimen.

(2). Use stub specimens in which the length of the reduced section of the standard specimen is made shorter, while the other dimensions remain unchanged, so that the overall length of the specimen doesn't exceed the plate thickness.

Drawbacks:

a. The length-to-diameter ratio of the reduced section may become too small, so that the test results are influenced by the end effects of the enlarged ends.

b. The material near the plate surfaces are not included in the gage length. The test results will therefore not be representative of the plate thickness in its entirety.

c. Because of the many different lengths of reduced sections, machine-shop automation cannot always be readily utilized with this specimen,

Advantages:

The specimen usually has the advantage of having a larger cross section and standard grip ends.

(3). Use tab specimens in which high-strength prolongations (tabs) are welded to the plate surfaces in order to obtain the sufficient length needed for a standard-size specimen.

Drawbacks:

a. The heat-affected zone can cause anomalies in the measured tensile properties.

b. The high strength prolongation may introduce end restraint effects.

c. Since the specimen requires equipment and personnel to prepare the tabs and to perform the welding, this may significantly increase the cost of testing.

Advantages:

The tab specimen offers the convenience of a standard-size specimen for machining and testing and, if necessary, allows for the positioning of the reduced section at any location within the plate thickness

2.3 Material

All tensile coupons for the present investigation were taken from the 3 in (76.2 mm) thick flange of a single piece of a W14 × 426 rolled wide flange of A572 Grade 50 Steel. Table 2.1 shows the mechanical properties reported on the mill certificate for this section, while Table 2.2 shows the chemical composition reported on the mill certificate. This shape was produced by a mill located in the United Kingdom.

Table 2.1 The Mechanical Properties Reported on Mill Certificate for W14 × 426.

yield stress	51,669 psi
tensile stress	74,310 psi
elongation (base on 8″ gage length)	20 %

Table 2.2 The Chemical Analysis Reported on the Mill Certificate

C.	Si.	Mn.	P.	S.	NB	V
0.170	0.342	1.100	0.022	0.023	0.040	0.004

Note: All Quantities Reported in % by Weight.

For specimens with welded prolongations, the prolongations were made from 1″×1″ (25.4 mm×25.4 mm) bars of AISI 1018 Cold Finished steel. This material has a minimum specified yield stress of 54 ksi. However, tensile tests conducted on a sample of the material actually used for the prolongations indicated an actual yield stress of 90 ksi. Since the ultimate tensile strength of the column flange test material was approximately 74 ksi, no yield of the prolongations was anticipated prior to fracture of the column flange material.

2.4 Specimen Description and Preparation

In this investigation, the tensile properties of the 3 in (76.2 mm) thick flange, both in the rolling direction and in the through-thickness direction, were measured with five different series of specimens. These five different series were designated "A" through "E" , and are summarized in Table 2.3. All of the coupons were circular in cross section, with a 0.5 in (12.7 mm) diameter gage section. The coupons were machined with unthreaded upset ends for gripping, as described later.

Table 2.3 Summary of Test Specimen

Specimen Series	Direction of Testing	Coupon Description
A	Rolling Direction	7″ long modified standard tensile coupon
B	Rolling Direction	3″ long sub-length tensile coupon
C	Rolling Direction	7″ long tensile coupon prepared using welded prolongations
D	Through-Thickness Direction	3″ long sub-length tensile coupon
E	Through-Thickness Direction	7″ long tensile coupon prepared using welded prolongations

As indicated in Table 2.3, the Type A, B, and C specimens measured the rolling direction properties, whereas Type D and E measured the through-thickness properties. The Type A specimens were 7 inches (177.8 mm) in length and oriented along the rolling direction. These specimens were intended to represent a modified standard 0.5 in (12.7 mm) diameter tensile coupons as a baseline. Specimen Type B and D were sub-length specimens, with a total length

of 3 inches (76.2 mm)(equal to the flange thickness), and a reduced section length of 1.5 inches (38.1 mm). Type B was oriented in the rolling direction and Type D in the through-thickness direction. Note that in the through-thickness direction, the Type D specimen only tests the middle portion of the flange, since the outer portions are included in the upset ends.

For the Type B and E specimens, 3 in (75 mm) long pieces of flange material were cut from the flange. High strength prolongations were then welded to these pieces to form a coupon with a total length of 7 inches (177.8 mm). For Type B specimens, the 3 in (75 mm) long piece of flange material was oriented in the rolling direction, while for Type E, it was oriented along the through-thickness direction. Specimens with welded prolongations are useful for thinner flanges, where a coupon cannot be machined directly from the flange in the through-thickness direction.

Eight coupons were prepared and tested for each of the five different types of specimens. Consequently, a total of 40 coupons were tested. The general orientation for each of the five types of specimens are shown in Figures 2.2 and 2.3. The geometry of each of the five types of specimens can formed with requirements of ASTM A770, except that a smaller radius was used at the ends of the reduced section at the transition to the enlarged ends. This smaller radius was used to simplify machining. No failures occurred at this transition region in any of the 40 coupons that were tested.

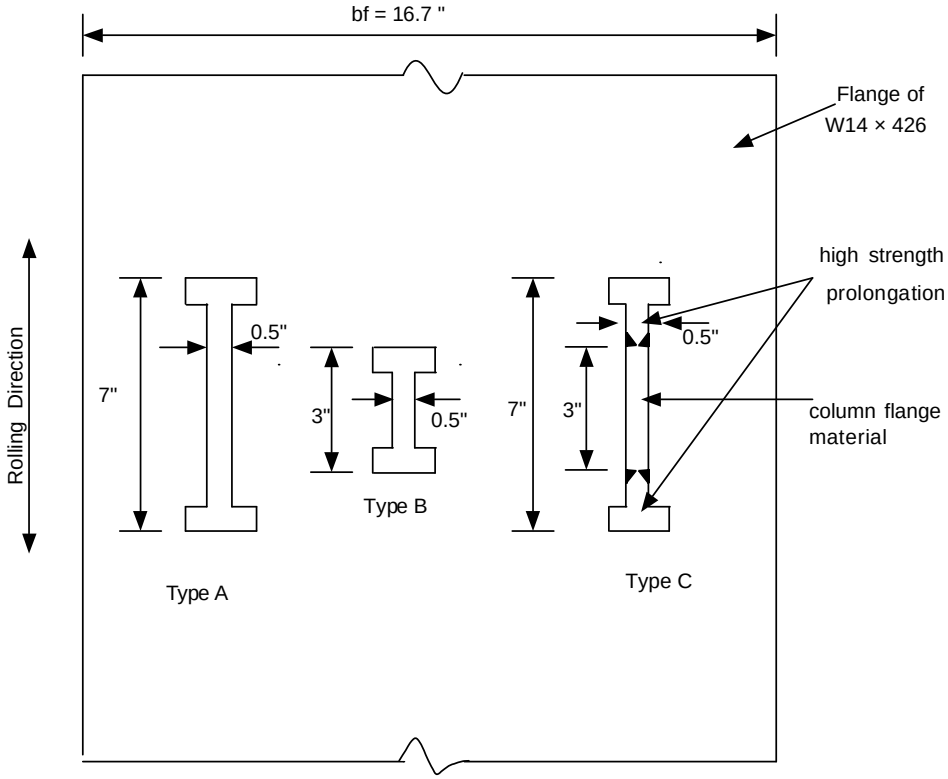

Fig 2.2 The Orientation of Specimen Types A, B and C

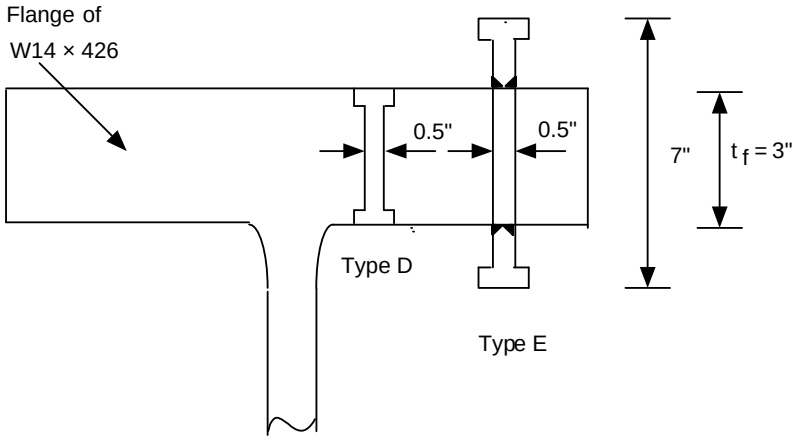

Fig 2.3 The Orientation of Specimen Types D and E

Each tensile coupon was machined from a rectangular blank, which was cut by a saw from the column flange. The location of the eight blanks for each of the 5 specimen types is shown in Figures 2.4 and 2.5. For any given specimen type, the eight blanks were taken across the width of the flange. In order to minimize the influence of possible material variation along the length of the member, the five different specimen types were taken immediately adjacent to one another along the length of the flange (Fig 2.5).

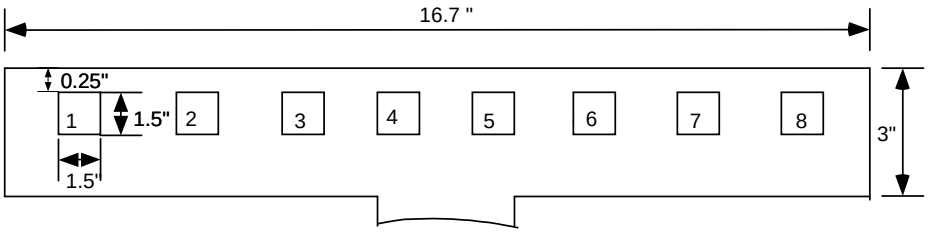

Fig 2.4a The Specimen Blank Location of Type A Specimens

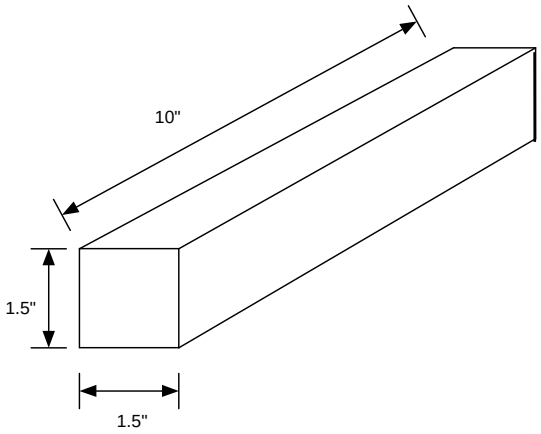

Fig 2.4b A Blank Configuration of Type A Specimens.

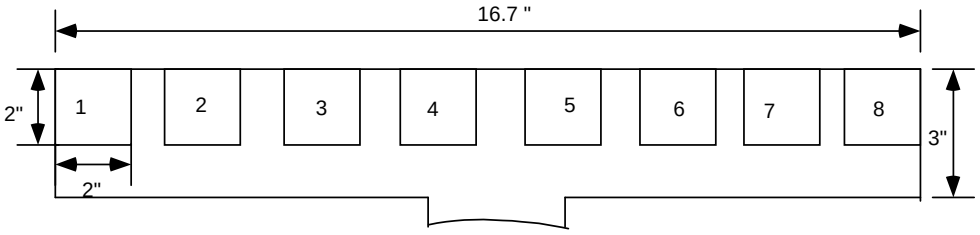

Fig 2.4c The Specimen Blank Location of Type B and Type C Specimens

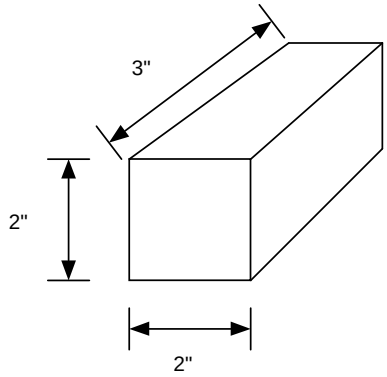

Fig 2.4d A Blank Configuration of Type B and Type C Specimens

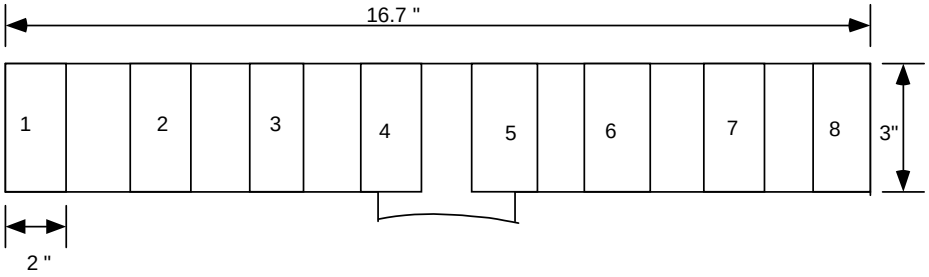

Fig 2.4e The Specimen Blank Location of Type D and Type E Specimens

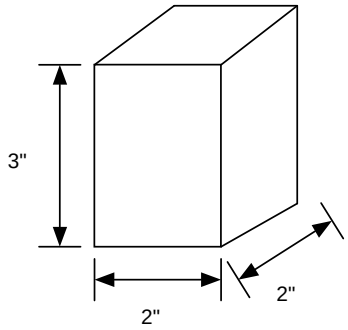

Fig 2.4f A Blank Configuration of Type D and Type E Specimens

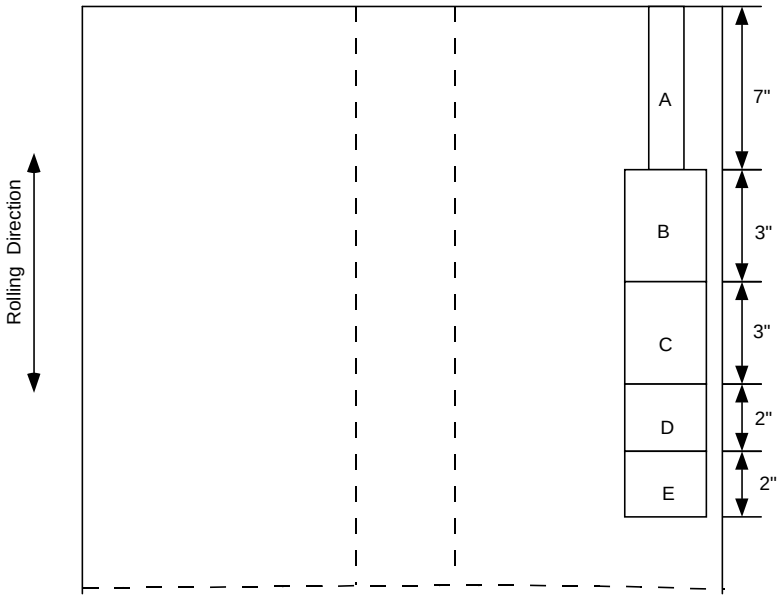

Fig 2.5 Specimen Location along the Rolling Direction of the Steel Column Flange

2.4.1 Type A Specimen

Type A Specimens are the 7-in (177.8-mm) long modified standard 0.5-in (12.7-mm)-diameter tensile coupons that are oriented in the rolling direction. First, a 1"×1"×10" (25.4 mm×25.4 mm×254 mm) rectangular blank was cut from the flange, and then machined to its final geometry. The Type A configuration is illustrated in Fig 2.6. In order to obtain meaningful comparative results, the geometry of the Type A specimen is the same as that used for the Type C and E specimens.

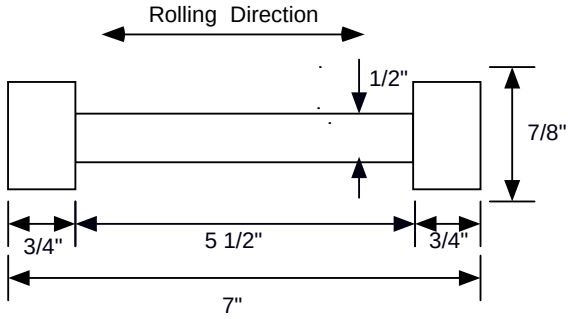

Fig 2.6 Type A Specimen Configuration.

2.4.2 Type B Specimen

Type B Specimens are the 3-in (76.2-mm) long sub-length 0.5-in (12.7-mm)-diameter tension coupons that are oriented in the rolling direction. The coupons here were machined from 2"×2"×3" (50.8 mm×50.8 mm×76.2 mm) blanks cut from the flange. The Type B configuration is illustrated in Fig 2.7.

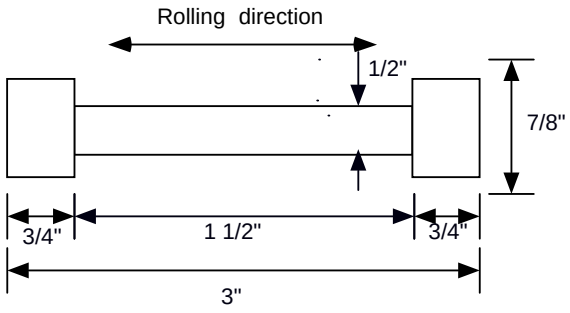

Fig 2.7 Type B Specimen Configuration

2.4.3 Type C Specimen

Type C Specimens were constructed using welded prolongations. These specimens were prepared by first cutting a 2"× 2"×3" (50.8 mm×50.8 mm×76.2 mm) steel blank along the rolling direction of the flange. Next, high-strength prolongations made of 1"×1"×4" (25.4 mm×25.4 mm×101.6 mm) bars were welded on to both surfaces . The coupon was then machined to the configuration shown in Fig 2.8. The coupon configuration was chosen in order to match coupon Type A.

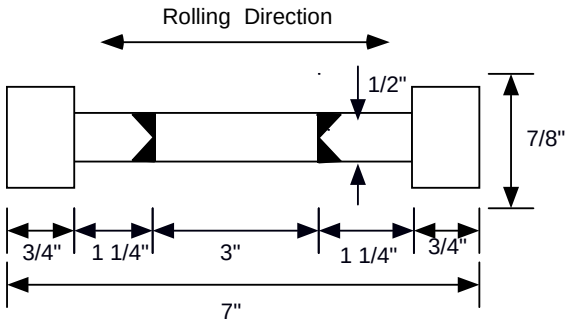

Fig 2.8 Type C Specimen Configuration

2.4.4 Type D Specimen

Type D specimens are the 3-in (76.2-mm) long 0.5-in (12.7-mm)-diameter tension coupons that are oriented along the through thickness direction of the flange. Full-thickness Z-direction tension specimen blanks, 2"× 2"×3" (50.8 mm×50.8 mm×76.2 mm), were cut from the steel column flange. The Type D specimens were machined directly from the tension specimen blanks without welding. The Type D configuration is illustrated in Fig 2.9, and is the same as in Type B configuration.

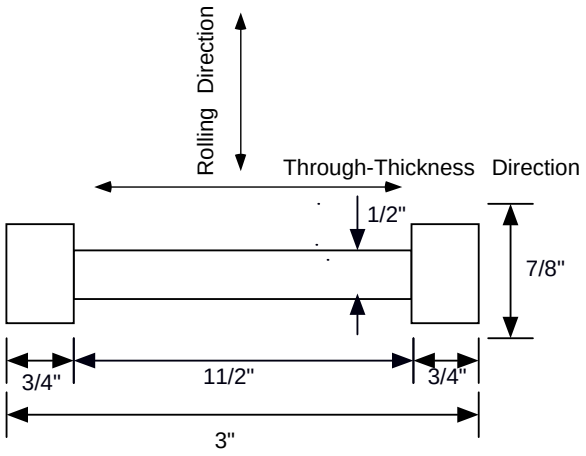

Fig 2.9 Type D Specimen Configuration

2.4.5 Type E Specimen

Type E Specimens were prepared using welded prolongation, similar to the procedure used in the Type C specimens. The 3-in (76.2-mm) long center section of the Type E coupons was oriented along the through-thickness direction. The configuration for Type E is shown in Fig 2.10, and is the same as in Type C.

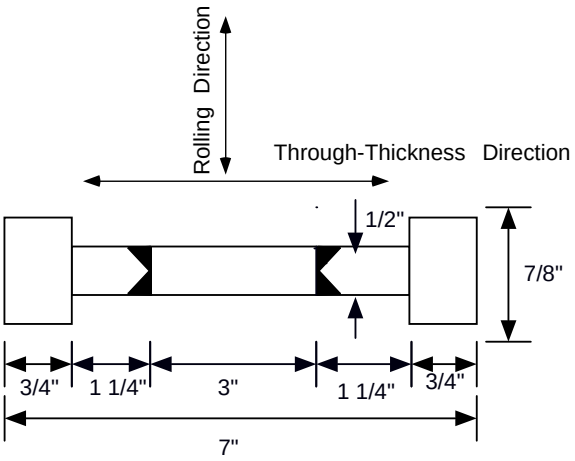

Fig 2.10 Type E Specimen Configurations

2.5 Slenderness Ratio

The slenderness ratio (L/d) for each specimen configuration is shown in Table 2.4. The L here is based on the entire reduced section length for Type A, B and D specimens and the 3" (76.2 mm) insert for Type C and E specimens. The d is based on the diameter of the reduced section. In order to allow for comparisons between the properties in the rolling direction and in the through-thickness direction, Types B and D were chosen so as to have the same configuration and slenderness ratio as well as Types C and E.

Table 2.4 Slenderness Ratio (L/d) for each Specimen Configuration

Specimen Type	A	B	C	D	E
L/d ratio	11	4.2	6	4.2	6

2.6 Welding Procedure

For Specimen Types C and E, the prolongations were welded to the column flange material using double bevel complete penetration groove welds, as shown in Fig 2.11. Weldings was accomplished by the shielded metal arc welding (SMAW) process, using E9018 electrodes. The material was preheated to 250°F prior to welding. The approximate weld bead sequence is shown in Fig 2.11. The equipment used for this welding did not permit monitoring of the welding voltage and current. Consequently, these welding parameters cannot be reported.

Prior to preparing Specimen Types C and E, several trial coupons were prepared and tested using the same materials and welding procedures as ultimately used for Specimen Types C and E. For each of these trial coupons, no failures occurred either in the weld nor in the prolongations. The necking and fracture occurred within the center section of the coupon , as intended.

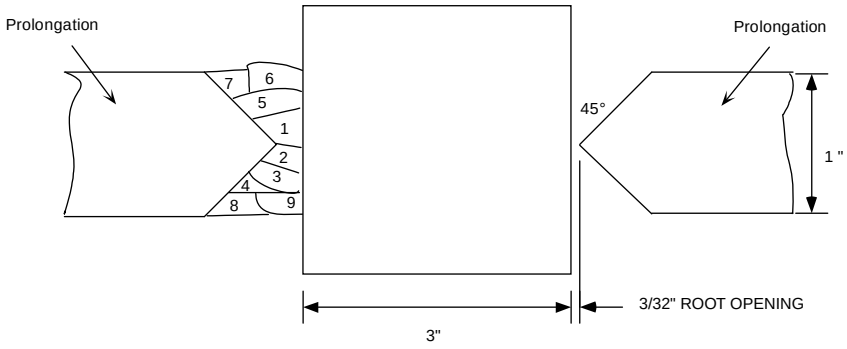

Fig 2.11 Weld Details

CHAPTER 3

TEST PROGRAM

3.1 Test Equipment

All tensile coupons were tested in a 120 Kip (533 kN) capacity test machine manufactured by Tinius-Olsen (Fig 3.1). This machine is screw driven, permitting control of cross-head speed and permitting accurate determination of static yield stress values.

Load on the test machine is read by a mechanical dial indicator on the machine. For the 7-in (177.8-mm) long coupons (Types A, C, E), an extensometer was attached at mid-length of the coupon in order to measure strain. The clip-on type extensometer was model S-100, manufactured by Tinius Olsen (Fig 3.2). This extensometer has a 2 inch (50.8 mm) initial gage length. During the testing of coupon types A, C and E, the strain measured by the extensometer and the load on the coupon were plotted on a pen plotter (Fig 3.3). After yield strength values were determined for each coupon, the extensometer was removed in order to avoid damage to the extensometer when the coupon fractured. Thus, only the initial portion of the stress-strain curves was recorded. For the 3 inch (76.2 mm) long coupons (Types B, D), there was inadequate space to fit the extensometer on to the coupon. Consequently, no extensometer readings were take on coupon Types B and D.

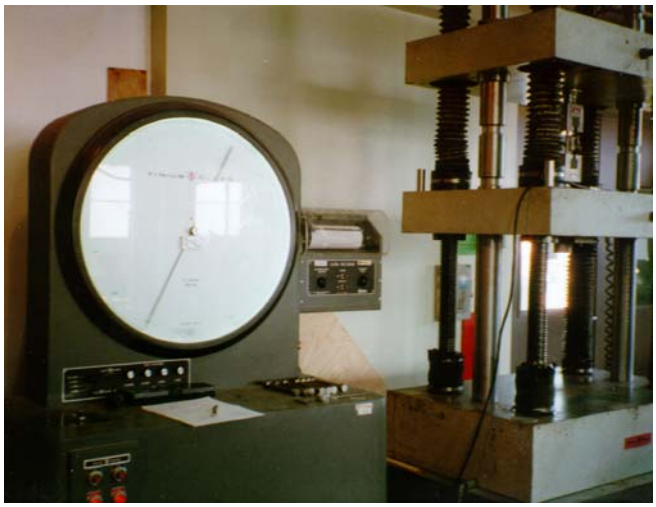

Fig 3.1 Tinius-Olsen Testing Machine

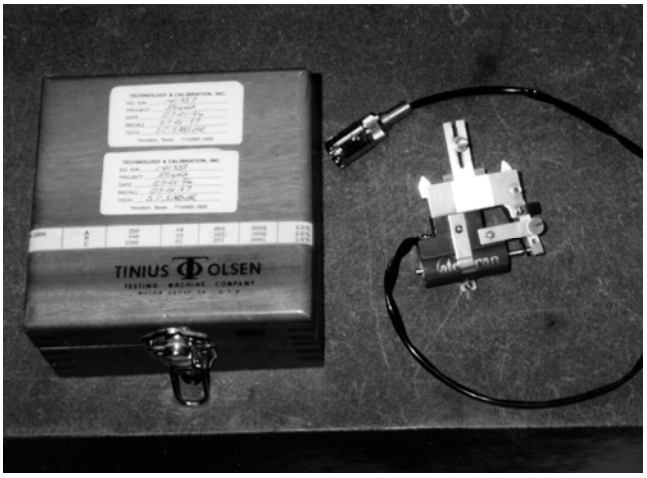

Fig 3.2 S-100 Tinius-Olsen Extensometer

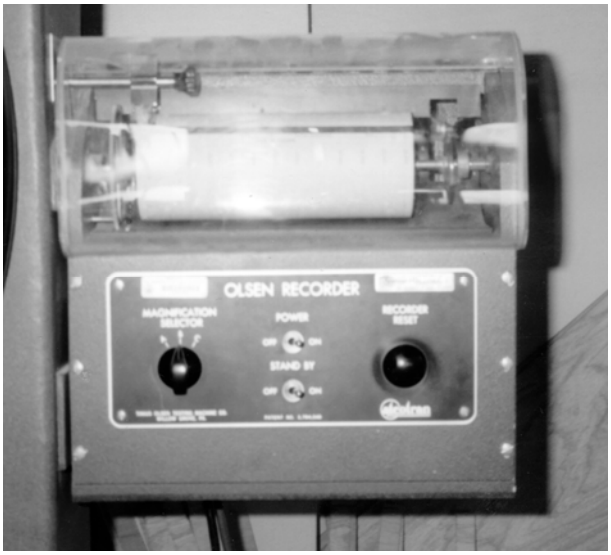

Fig 3.3 Tinius-Olsen Model 51 Recorder

Round tensile specimens are commonly gripped using threaded ends. For this test program, however, a coupon with enlarged shoulder ends was used rather than a coupon with threaded ends. Typical coupons, prior to testing, are shown in Figs 3.4 and 3.5. The simpler enlarged ends were used in lieu of threaded ends to simplify the machining of the coupons. The specimens were gripped using a sliding block specimen holder manufactured by Tinius Olsen, as shown in Fig 3.6. Figures 3.7 and 3.8 show specimens mounted in the specimen holder prior to testing. Figures 3.9 and 3.10 show specimens in the specimen holder after fracture of the coupons.

Fig 3.4 A Type A Specimen (The Same Configuration as Types C, E Specimens) before Testing

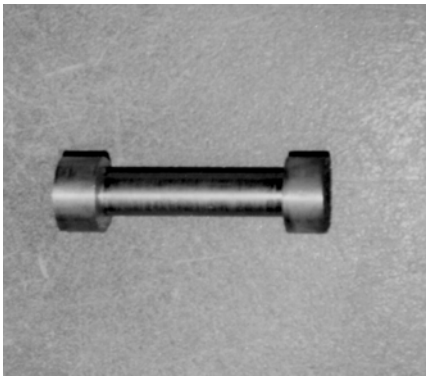

Fig 3.5 A Type B Specimen (The Same Configuration as Type D specimens) before Testing.

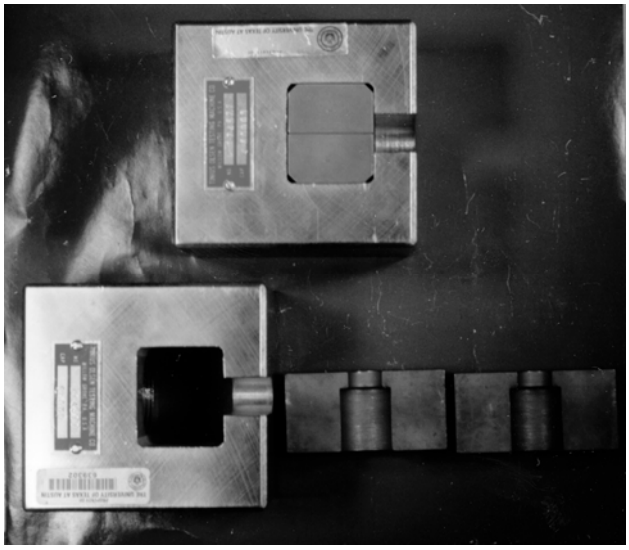

Fig 3.6 Tinius-Olsen Block Type Headed Specimen Holders

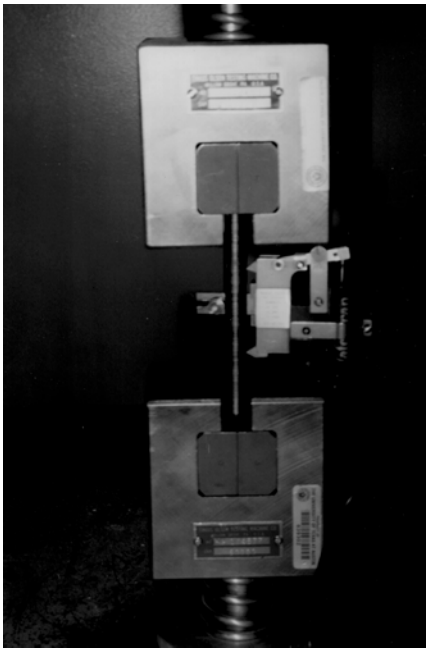

Fig 3.7 Type A Specimen Mounted in Specimen Holder, with Extensometer.

Fig 3.8 Type B Specimen in Specimen Holder.

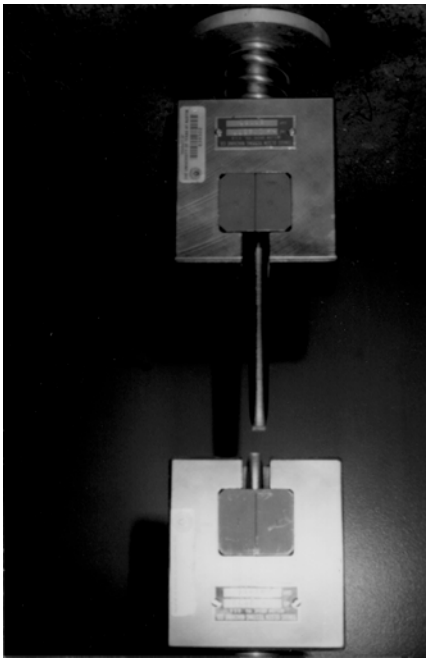

Fig 3.9 Type A Specimen at End of Test

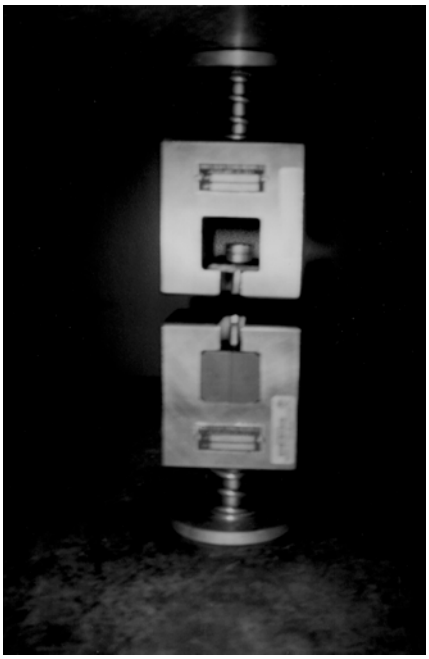

Fig 3.10 Type B Specimen at End of Test

3.2 Definition of Terms

In this section, several terms that are used throughout this report are described. These terms are related to the interpretation of a tensile test.

Figure 3.11 shows, qualitatively, the initial part of a stress-strain plot for a typical structural steel. When yielding first occurs, an upper yield point is sometimes exhibited. After passing the upper yield point, if one exists, the stress then remains reasonably constant at the " dynamic yield stress" value until the onset of strain hardening, as shown in Fig 3.11. The value of the dynamic yield stress, which is read while the test machine cross-heads are in motion, depends on

the applied strain rate. Generally, higher strain rates result in higher dynamic yield stress values.

Within the yield plateau region, if the cross-heads are stopped and held at a constant position, i.e., the coupon is held at a constant strain level, the stress on the coupon will reduce, as shown in Fig 3.11. After several minutes, the stress will stabilize at the "static" yield stress value. The static yield stress corresponds to the yield stress at a zero strain rate. For these tests, static yield stress values were taken after a period of 5 minutes, following the time at which the cross-heads were stopped. Screw driven test machines, such as the Tinius-Olsen machine used for these tests, are particularly useful for obtaining static yield points. Screw driven machines can reliably hold the coupon at constant strain. Obtaining static yield stress values with hydraulically driven test machines can be more difficult, since small leaks in the hydraulic valves can result in a change in strain. It is for this reason that the screw driven Tinius-Olsen test machine was chosen for this test program.

After the static yield stress value is determined, if the machine cross-heads are again set into motion, the stress will increase to the dynamic yield stress value. As before, the value of the dynamic yield stress depends on the applied strain rate.

For these tests, generally three static yield stress values were taken within the yield plateau region. The final reported value of static yield stress is the average of these three. Similarly, three dynamic yield stress values were generally taken within the yield plateau, and then averaged. All three dynamic yield stress values were taken with the cross-heads running at the same rate.

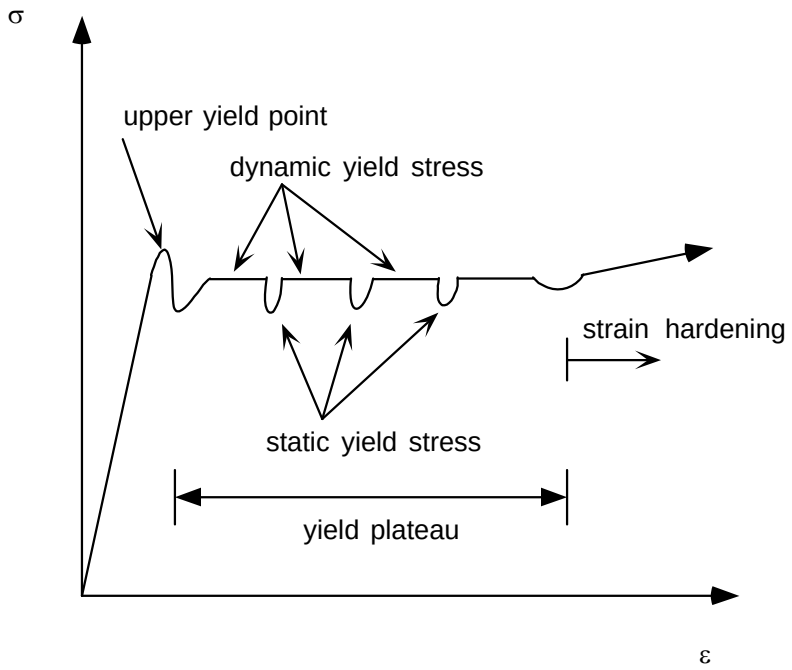

Fig 3.11 Qualitative Representation of Initial Portion of Stress-Strain Plot

For the 7 in (177.8 mm) long coupons, static and dynamic yield stress values were taken from the load versus strain plots recorded during the test. For the 3 in (76.2 mm) long coupons, load versus strain plots were not available, since the extensometer could not be fit onto the coupon (Types B and D). For these coupons, the static and dynamic yield stress values were estimated from the load dial indicator on the test machine. This process requires some judgment in interpreting the movement of the load dial indicator. Consequently, static and dynamic yield stress values for the short coupons are somewhat less certain than for the longer coupons.

After leaving the yield plateau region, the stress-strain curve then enters the strain hardening region. The largest value of stress achieved during the course of the test is the ultimate stress, also referred to as the tensile strength. The value

of the ultimate stress is also strain rate dependent. Consequently, it is also possible to determine static and dynamic ultimate stress values. Static values can be determined by holding the coupon at constant strain for some period of time. For the present tests, only dynamic ultimate stress values were determined. These values represent the maximum stress on the coupons while the cross-heads were in motion. After achieving the ultimate stress, the stress decreases until fracture of the coupon occurs.

In addition to establishing yield and ultimate stress values, the percent elongation and the percent reduction in area were also determined from these tensile tests. Both of these quantities are a measure of ductility.

To determine the percent elongation, small gage marks are punched on the coupon prior to testing. These marks are typically placed either 2 inches or 8 inches apart. At the completion of the test, the fractured coupon is held together, and the final distance between the punch marks is measured. The percent elongation is then computed as the change in length between the punch marks divided by the initial length, multiplied by 100. Note that the percent elongation represents the engineering strain (expressed as a percentage) at fracture of the coupon.

To determine the present reduction in area, the diameter of the coupon is carefully measured prior to testing. The initial area of the coupon is then computed. At the completion of the test, the diameter of the minimum section at the fracture is measured, from which the final area is computed. The percent reduction in area is then computed as the change in area, multiplied by 100.

To summarize, the key quantities measured in these tests are defined below:

- Static Yield Stress ($F_{y\text{-}static}$): The value of stress within the yield plateau region, determined with the coupon held at constant strain (no machine cross-head movement) for a period of 5 minutes. The reported value of $F_{y\text{-}static}$ represents the average of three static yield stress readings.

- Dynamic Yield Stress ($F_{y\text{-}dyn}$): The value of stress within the yield plateau region, determined while the machine cross-heads are in motion. All dynamic yield stress values were taken at a machine cross-head rate of 0.02 inches/minute. The reported value of $F_{y\text{-}dyn}$ represents the average of three dynamic yield stress readings.

- Dynamic Ultimate Stress ($F_{u\text{-}dyn}$): The maximum value of stress achieved during the tensile test, read while the machine cross heads are in motion. All dynamic ultimate stress values were taken at a machine cross-head speed of 0.02 inches/minute.

(Note: All stress values were computed as engineering stress, i.e., computed as the load on the coupon, divided by the initial area of the coupon.)

- Percent elongation (%EL):

$$\%EL = \frac{L_{final} - L_0}{L_0} \times 100$$

Where:

L_0 = initial length between punch marks on coupon (L_0 = 2 inches for all coupons)

L_{final}= final length between punch marks on coupon at completion of the test.

- Percent reduction in area (%RA):

$$\%RA = \frac{A_{final} - A_0}{A_0} \times 100$$

Where:

A_0 = initial cross-sectional area of coupon.

A_{final}= final cross-sectional area of coupon at the point of minimum area.

3.3 Test Procedure

Following is a summary of the procedure used to test the coupons.

1. Measure initial diameter of coupons. (Several measurements were taken and averaged). Compute initial area of coupon, A_0.

2. Punch gage marks approximately 2 inches apart, at mid-length of coupon. Measure exact distance between punch marks (= L_0)
3. Install coupon in sliding block grips in 120 kip (533 kN) Tinius-Olsen Test Machine.
4. Install extensometer on coupon and set up plotting paper to record load and strain (coupon Types A, C and E only).
5. Begin loading coupon. Use constant cross-head speed of 0.02 inches/minute for entire duration of test, except when determining static yield stress values.
6. After coupon is on yield plateau, stop test machine and wait 5 minutes. Take static yield load reading.
7. After taking static yield load value, resume cross-head movement at 0.02 inches/minute. After load has stabilized on yield plateau, take dynamic yield loading reading.
8. Repeat steps 6 and 7 two additional times, to obtain two additional readings of static and dynamic yield load values.
9. Take an average of the three static yield load values, and then divide by A_0 to obtain $F_{y\text{-}static}$
10. Take an average of the three dynamic yield load values, and then divide by A_0 to obtain $F_{y\text{-}dyn}$.
11. Remove extensometer (Coupon Types A, C and E).
12. Continue loading at 0.02 inches/minute until fracture of coupon.
13. Read maximum load achieved during test from test machine. Divide by A_0 to compute $F_{u\text{-}dyn}$.
14. Remove fractured coupon from grips. Measure final distance between punch marks, and final diameter at the minimum necked down region of the coupon. Compute %EL and %RA.

CHAPTER 4

RESULTS AND DISCUSSION

4.1 Introduction

The results of the tensile tests are presented and discussed in this chapter. The comparisons among the different specimen types are presented in terms of strength level, ductility level and the location of the specimen. In each case, the comparisons are divided into three categories: comparisons of specimens in the rolling direction; comparisons of specimens in the through-thickness direction; and comparison among all specimens.

4.2 Strength Level Results

In this section, static yield stress ($F_{y\text{-}static}$), dynamic yield stress ($F_{y\text{-}dyn}$) and dynamic ultimate stress ($F_{u\text{-}dyn}$) measurements are reported. Procedures used to determine these quantities were described in Chapeter 3. Figures 4.1 through 4.3 show typical load-strain curves recorded for each of the 7 inch (177.8 mm) long specimen types (Types A,C,E) for which an extensometer could be used. These plots illustrate the three static yield point readings, as described in Chapter 3. Note that these coupons exhibited a well defined yield plateau, both in the rolling and through thickness directions.

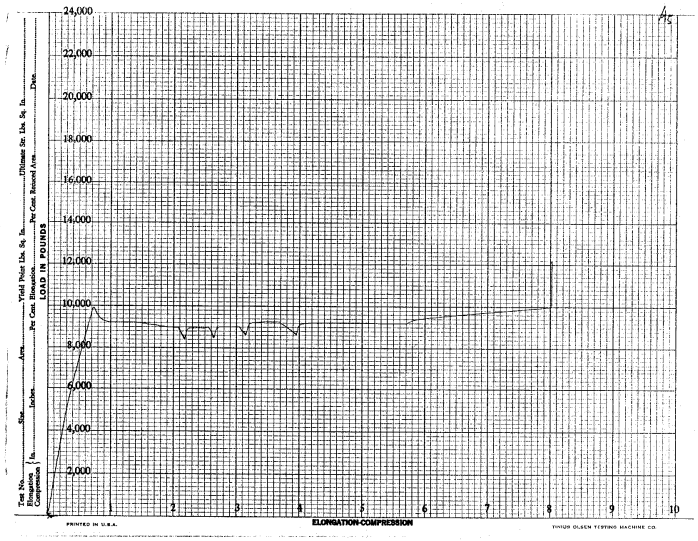

Fig 4.1 The Load-Strain Curve for Specimen A5

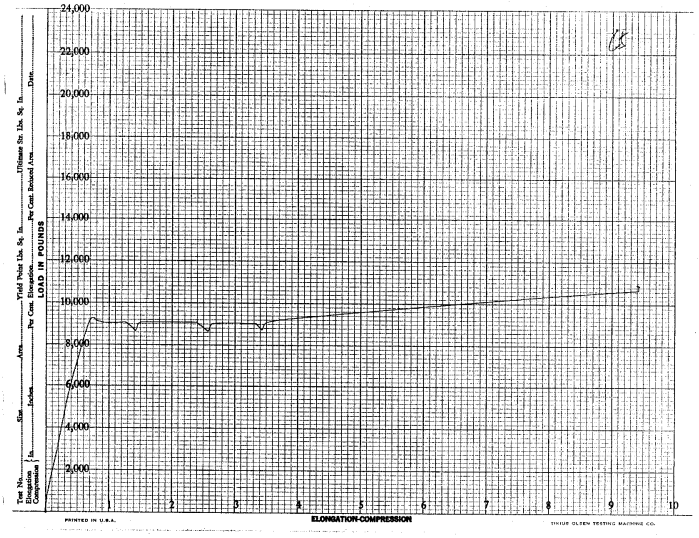

Fig 4.2 The Load-Strain Curve for Specimen C5

Fig 4.3 The Load-strain curve for specimen E5

4.2.1 Comparison of Specimens in the Rolling Direction

The strength properties in the rolling direction of specimen Types A, B and C are given in Tables 4.1 through 4.3, and are compared in Figures 4.4 through 4.6. The results for the individual specimens are plotted in Figures 4.7 through 4.15. The Type A specimens are the 7-in (177.8-mm) long modified standard tension coupons that are in the rolling direction. The Type B specimens are the 3-in (76.2-mm) long sub-length tensile coupons that are in the rolling direction. The Type C specimens are the 7-in (177.8-mm) long tensile coupons that were prepared using welded prolongations in the rolling direction. Standard deviations (STDEV) were computed here so that a comparison of specimen-to-specimen variability could be done.

Table 4.1 Comparison of the Static Yield Stress for Specimen Types A, B and C (ksi)

$F_{y\text{-static}}$	Types		
Specimen No.	A	B	C
1	47.10	49.03	48.92
2	44.76	43.12	44.76
3	44.13	42.53	43.22
4	42.38	41.16	43.35
5	42.43	42.13	43.65
6	43.98	43.62	43.72
7	44.18	44.81	44.59
8	49.40	47.00	56.70
Average	44.80	44.18	46.11
STDEV	2.37	2.66	4.66

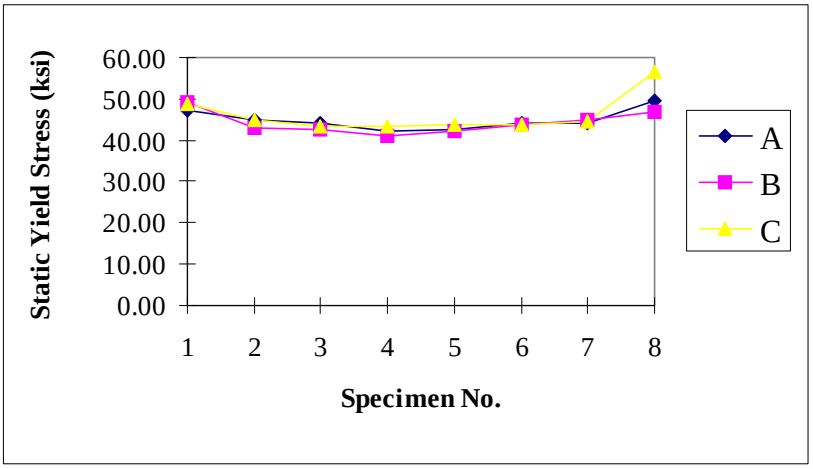

Fig 4.4 Comparison of the Static Yield Stress for Specimen Types A, B and C (ksi)

Table 4.2 Comparison of the Dynamic Yield Stress for Specimen Types A, B and C (ksi)

$F_{y\text{-}dyn}$	Types		
Specimen No.	A	B	C
1	51.19	61.20	52.08
2	48.20	47.16	47.82
3	47.12	44.84	46.58
4	48.67	44.00	45.99
5	44.97	44.43	46.84
6	47.50	46.56	47.73
7	47.51	47.03	48.36
8	52.34	49.67	59.59
Average	48.44	48.11	49.37
STDEV	2.34	5.60	4.53

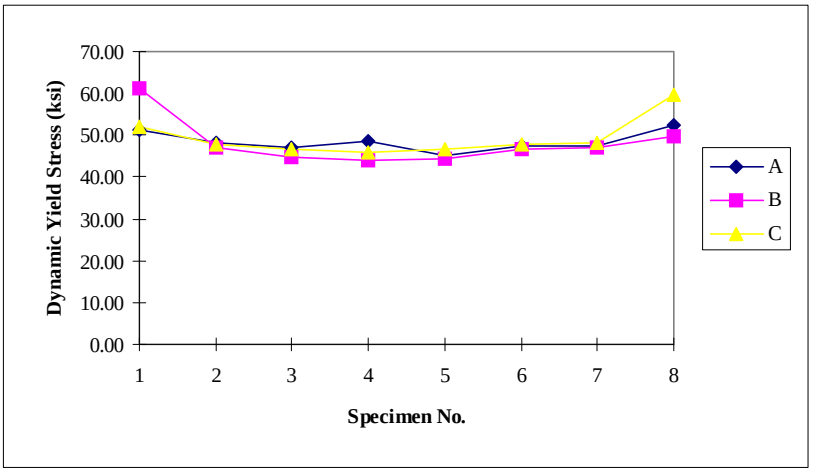

Fig 4.5 Comparison of the Dynamic Yield Stress for Specimen Types A, B and C (ksi)

Table 4.3 Comparison of the Dynamic Ultimate Stress for Specimen Types A, B and C (ksi)

$F_{u\text{-}dyn}$	Types		
Specimen No.	A	B	C
1	71.54	73.70	72.82
2	72.45	73.12	72.59
3	71.75	72.89	71.83
4	70.84	71.71	71.60
5	70.91	72.67	72.42
6	71.35	73.01	72.42
7	71.42	73.06	72.48
8	72.12	72.07	71.58
Average	71.55	72.78	72.22
STDEV	0.55	0.63	0.48

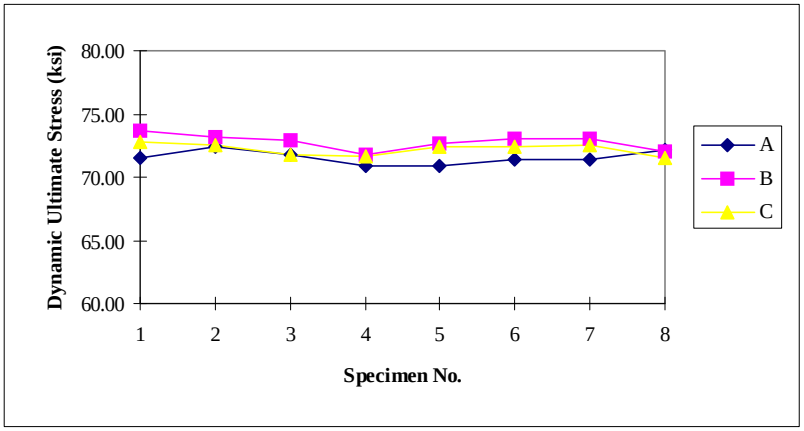

Fig 4.6 Comparison of the Dynamic Ultimate Stress for Specimen Types A, B and C (ksi)

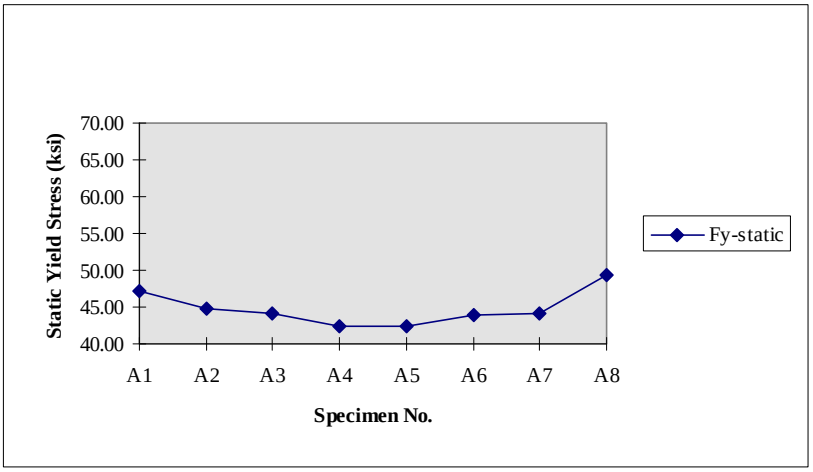

Fig 4.7 The Static Yield Stress for Type A Specimens (ksi)

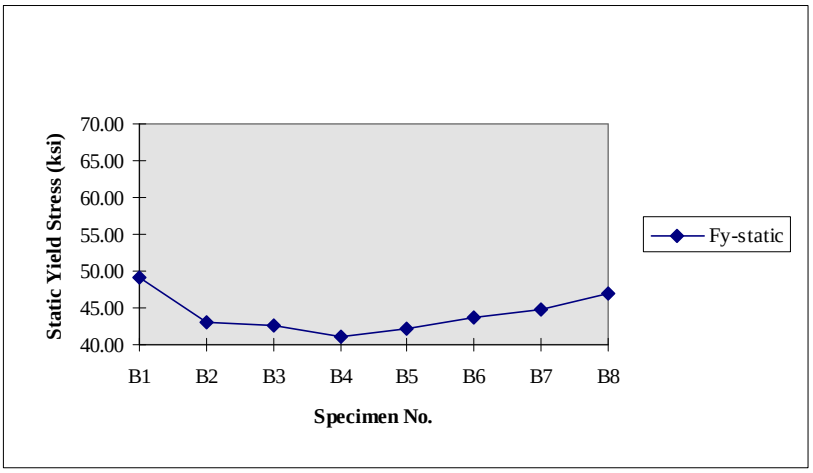

Fig 4.8 The Static Yield Stress for Type B Specimens (ksi)

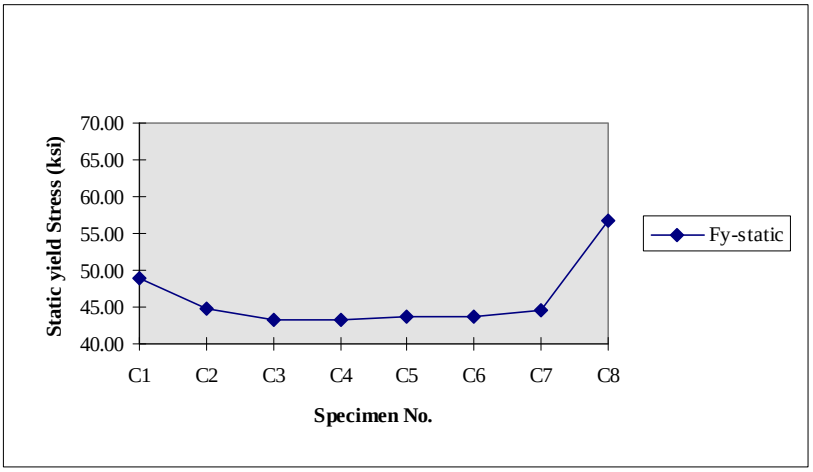

Fig 4.9 The Static Yield Stress for Type C Specimens (ksi)

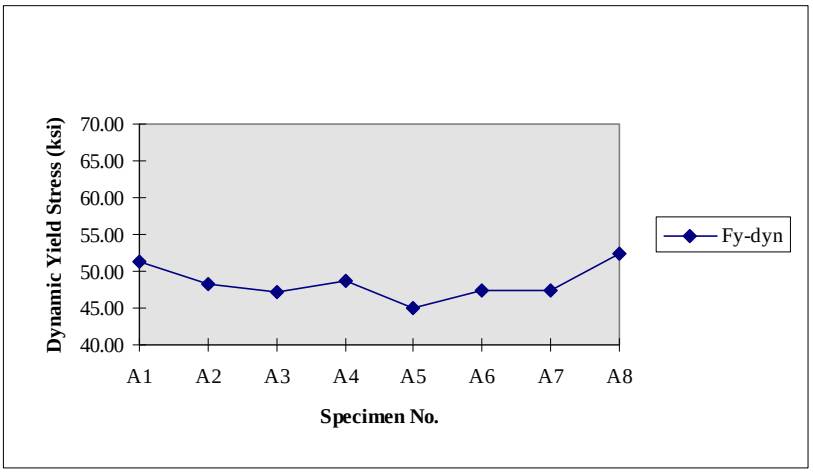

Fig 4.10 The Dynamic Yield Stress for Type A Specimens (ksi)

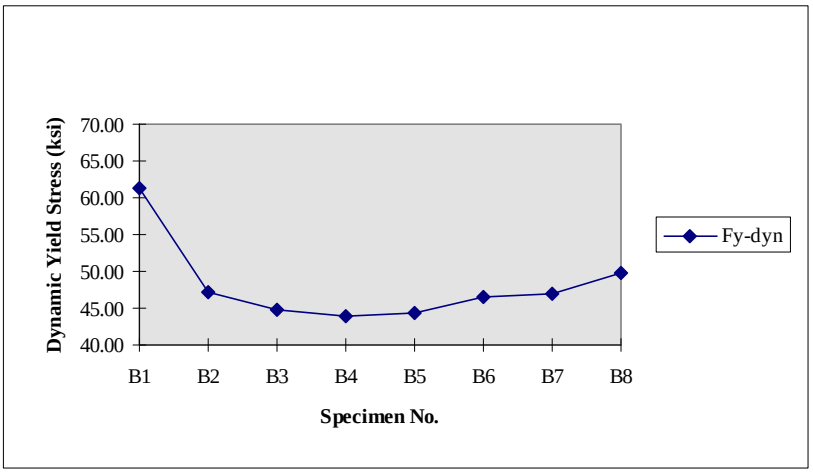

Fig 4.11 The Dynamic Yield Stress for Type B Specimens (ksi)

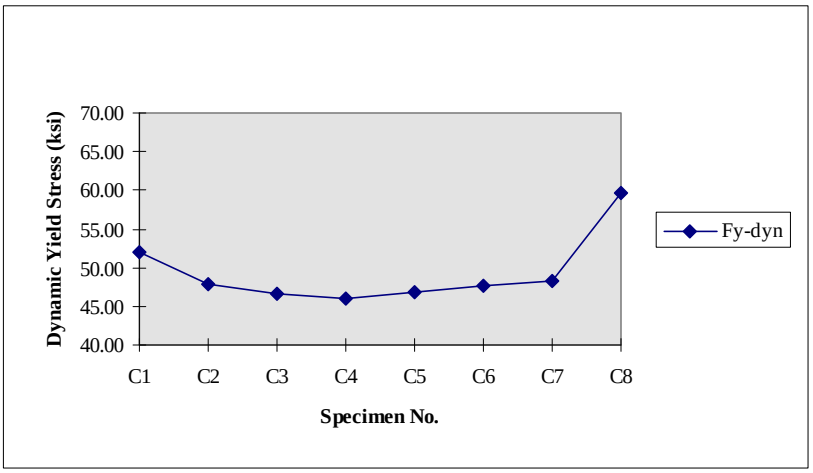

Fig 4.12 The Dynamic Yield Stress for Type C Specimens (ksi)

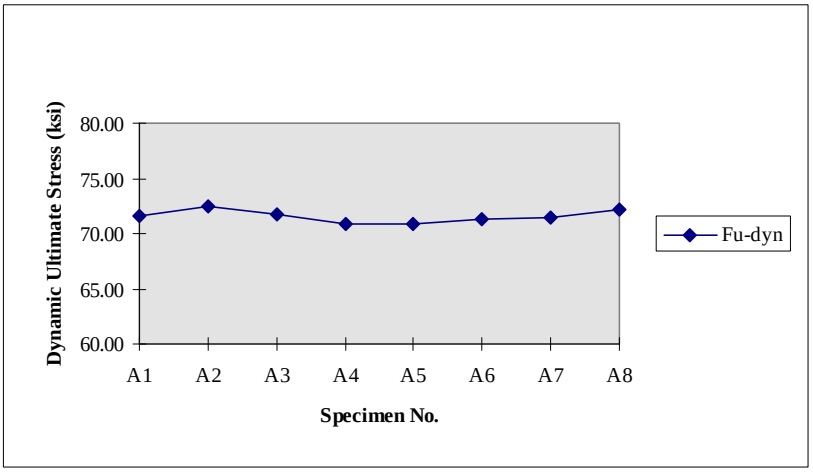

Fig 4.13 The Dynamic Ultimate Stress for Type A Specimens (ksi)

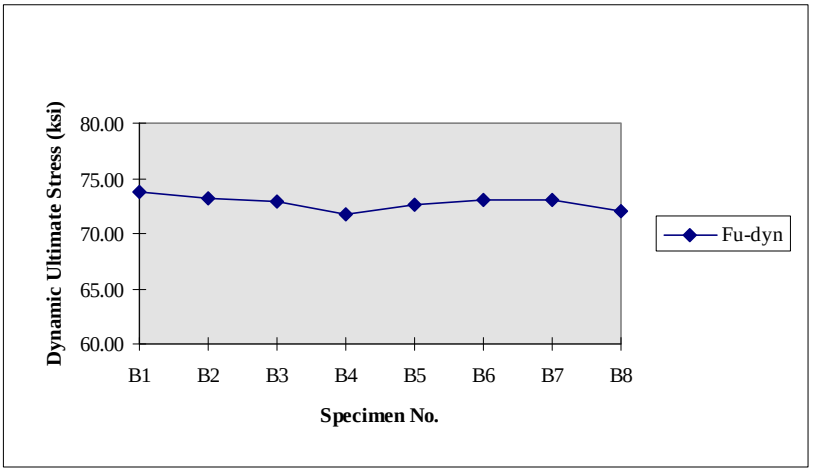

Fig 4.14 The Dynamic Ultimate Stress for Type B Specimens (ksi)

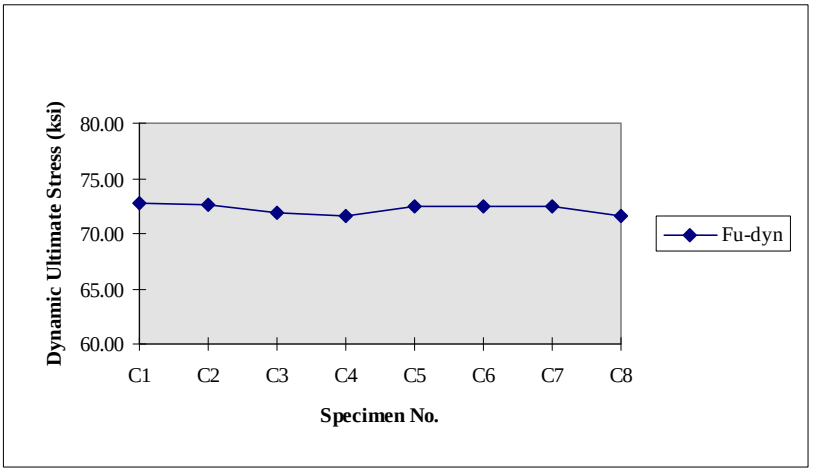

Fig 4.15 The Dynamic Ultimate Stress of Type C Specimens (ksi)

These results show little difference in yield or ultimate stress values measured for the three different types of coupons. The static and dynamic yield stress values for Specimen Type B were determined directly from the load dial indicator, since this specimen was too short to permit the use of an extensometer. For Specimen Type A, on the other hand, static and dynamic yield stress values were determined from the recorded stress strain plot, as described in Chapter 3. The close agreement of the static and dynamic yield stress for Specimen Types A and B indicate the procedures used to determine yield stress values for specimen Type B provided good results.

Specimen Type C, prepared using welded prolongations, showed slightly higher static and dynamic yield stress values than Type A and B. The differences, however, are small. For the average of eight coupons, the static and dynamic yield stress values were about 1 to 2 ksi higher for Type C. This may reflect a small influence of the welding, or may simply reflect variability in the test results.

All three coupon types showed nearly identical ultimate stress values. The variability in the ultimate stress measurements was significantly smaller than for the yield stress measurements, as reflected in the standard deviation results.

Overall, these results suggest that all three coupon types give comparable results for static yield stress, dynamic yield stress, and dynamic ultimate stress in the rolling direction.

Finally, these results indicate that the material near the outer edges of the column flange are somewhat higher in strength than the material near the center of the flange. The trend is more pronounced for yield stress than for ultimate stress.

4.2.2 Comparison of Specimens in the Through-Thickness Direction

The strength properties in the through-thickness direction for Specimen Types D and E are given in Tables 4.4 through 4.6. The properties for the Type A specimens are also shown, as a reference. Trends in the strength properties in the through-thickness direction are illustrated in Figures 4.16 through 4.18, while the results for the individual specimens are depicted in Figures 4.19 through 4.22.

Table 4.4 Comparison of the Static Yield Stress for Specimen Types A, D and E (ksi)

$F_{y\text{-static}}$	Types		
Specimen No.	A	D	E
1	47.10	47.58	60.55
2	44.76	42.95	60.80
3	44.13	42.29	59.65
4	42.38	41.20	60.13
5	42.43	42.14	61.26
6	43.98	42.34	62.00
7	44.18	42.99	62.45
8	49.40	45.63	59.62
Average	44.80	43.39	60.81
STDEV	2.37	2.12	1.04

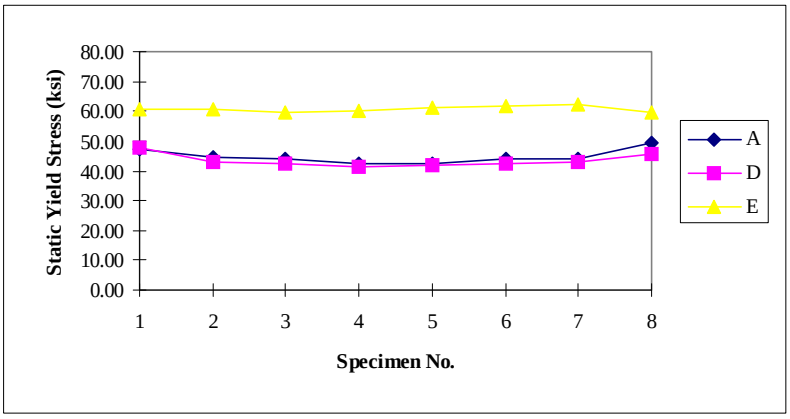

Fig 4.16.Comparison of the Static Yield Stress for Specimen Types A, D and E (ksi)

Table 4.5 Comparison of Dynamic Yield Stress for Specimen Types A, D and E (ksi)

$F_{y\text{-}dyn}$	Types		
Specimen No.	A	D	E
1	51.19	50.73	63.52
2	48.20	45.64	63.81
3	47.12	44.54	62.65
4	48.67	43.76	63.18
5	44.97	44.58	64.24
6	47.50	44.55	65.17
7	47.51	45.37	65.71
8	52.34	48.28	62.26
Average	48.44	45.93	63.82
STDEV	2.34	2.37	1.19

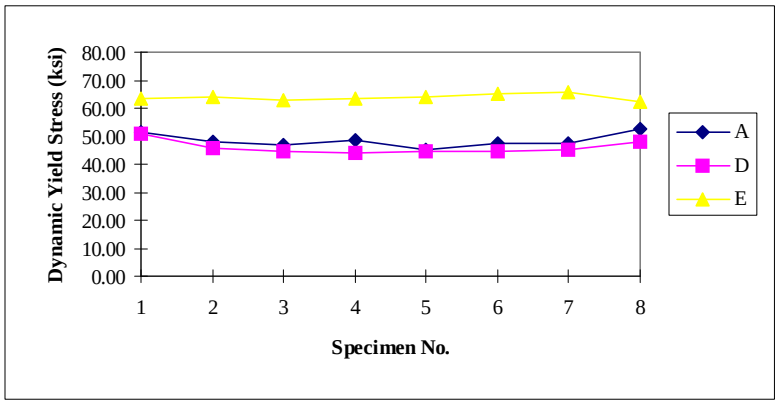

Fig 4.17 Comparison of Dynamic Yield Stress for Specimen Types A, D and E (ksi)

Table 4.6 Comparison of Dynamic Ultimate Stress for Specimen Types A, D and E (ksi)

$F_{u\text{-}dyn}$	Types		
Specimen No.	A	D	E
1	71.54	72.50	70.17
2	72.45	70.75	69.53
3	71.75	70.32	68.30
4	70.84	69.06	66.90
5	70.91	70.29	68.30
6	71.35	70.77	69.25
7	71.42	71.02	70.68
8	72.12	71.18	69.48
Average	71.55	70.74	69.08
STDEV	0.55	0.97	1.20

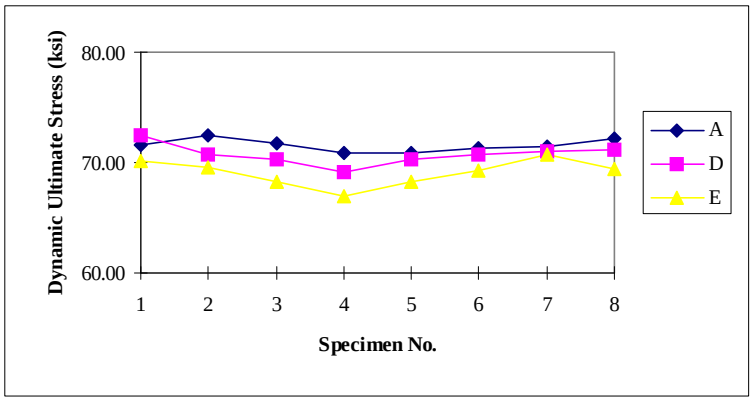

Fig 4.18 Comparison of Dynamic Ultimate Stress for Specimen Types A, D and E (ksi)

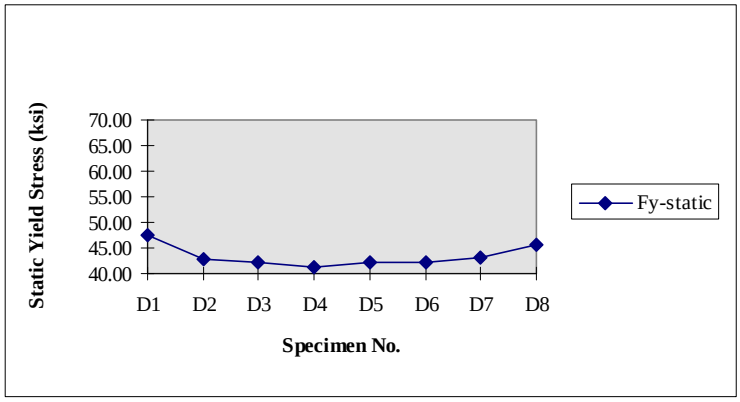

Fig 4.19 Static Yield Stress for Type D Specimens

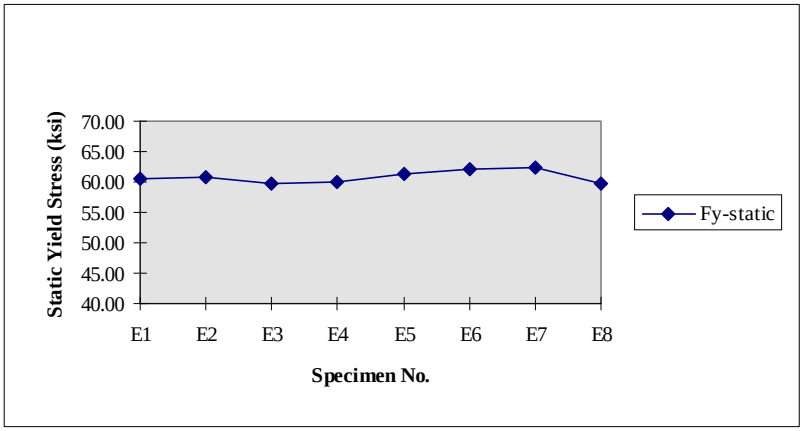

Fig 4.20 Static Yield Stress for Type E Specimens

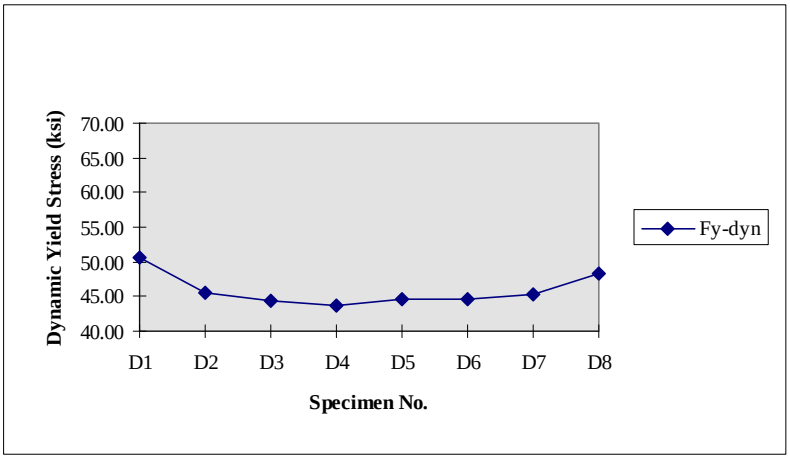

Fig 4.21 Dynamic Yield Stress for Type D Specimens

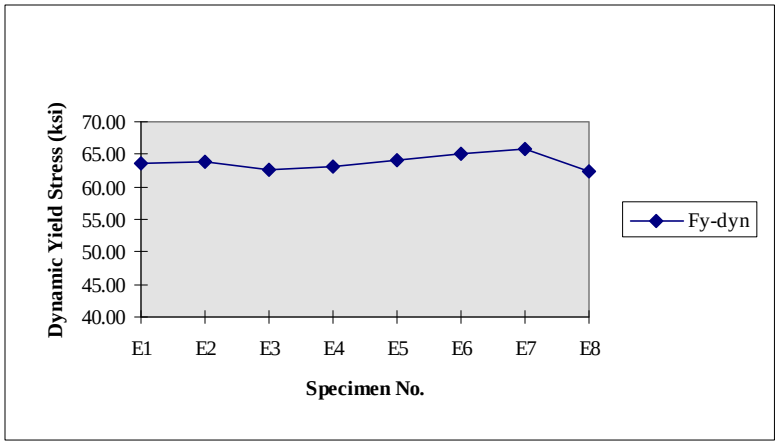

Fig 4.22 Dynamic Yield Stress for Type E Specimens

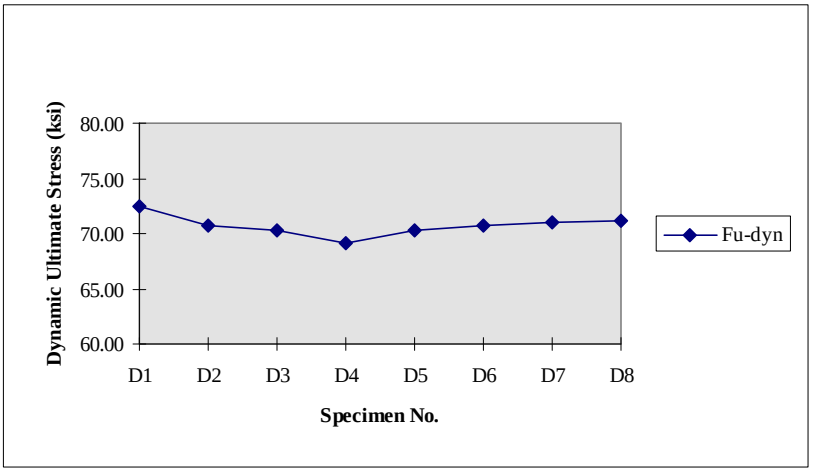

Fig 4.23 Dynamic Ultimate Stress for Type D Specimens

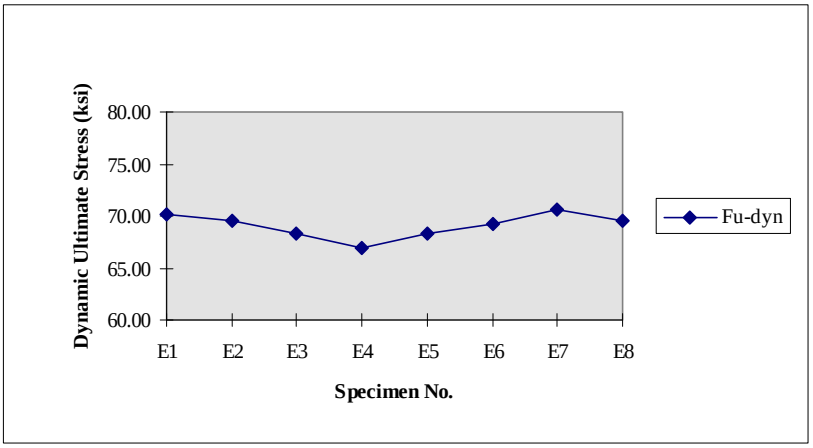

Fig 4.24 Dynamic Ultimate Stress for Type E Specimens

Specimen Type E, prepared using welded prolongations, showed much higher static and dynamic yield stress values than Types A and D. Since the slenderness ratio for Specimen Type E is 6 and the insert section for Specimen

Type E is 3 in (76.2 mm), the high strength welding should not significantly affect the strength result. Furthermore, similar high values of yield stress were not observed for the specimens with welded prolongations in the rolling direction (Specimen Type C). Consequently, the reason for the unexpectedly high yield stress values for Specimen Type E is unknown.

Specimen Type D, the 3 in (76.2 mm) long sub-length coupons, showed nearly identical results to Specimen Type A in terms of static yield stress values. There is only about 1 to 2 ksi difference between these two specimen types except specimens A8 and D8 which had about 4 ksi difference.

These three specimen types showed good agreement in the measured dynamic ultimate stress. This suggests that Specimen Types D and E can give comparable dynamic ultimate stress results in the through-thickness direction.

In terms of the standard deviation results, Specimen Type E showed slightly higher variability in dynamic ultimate stress than in the static and dynamic yield stress. This result is opposite to the results from Specimen Types A and D.

As was the case in the rolling direction, the material near the outer edges of the column flange showed somewhat higher through-thickness strength than the material near the center of the flange.

4.2.3 Comparison of All Specimens

The comparison of the tensile specimens in the rolling direction (Types B and C) with the tensile specimens in the through-thickness direction (Types D and E) are shown in Tables 4.7 through 4.12. The trend of the tensile properties are graphically depicted in Figures 4.25 through 4.30.

Table 4.7 Comparison of the Static Yield Stress for Specimen Types A, B and D (ksi)

$F_{y\text{-static}}$	Types		
Specimen No.	A	B	D
1	47.10	49.03	47.58
2	44.76	43.12	42.95
3	44.13	42.53	42.29
4	42.38	41.16	41.20
5	42.43	42.13	42.14
6	43.98	43.62	42.34
7	44.18	44.81	42.99
8	49.40	47.00	45.63
Average	44.80	44.18	43.39
STDEV	2.37	2.66	2.12

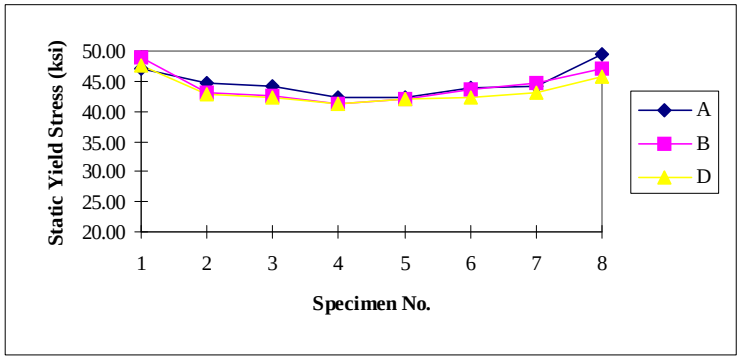

Fig 4.25 Comparison of the Static Yield Stress for Specimen Types A, B and D (ksi)

Table 4.8 Comparison of the Dynamic Yield Stress for Specimen Types A, B and D (ksi)

$F_{y\text{-}dyn}$	Types		
Specimen No.	A	B	D
1	51.19	61.20	50.73
2	48.20	47.16	45.64
3	47.12	44.84	44.54
4	48.67	44.00	43.76
5	44.97	44.43	44.58
6	47.50	46.56	44.55
7	47.51	47.03	45.37
8	52.34	49.67	48.28
Average	48.44	48.11	45.93
STDEV	2.34	5.60	2.37

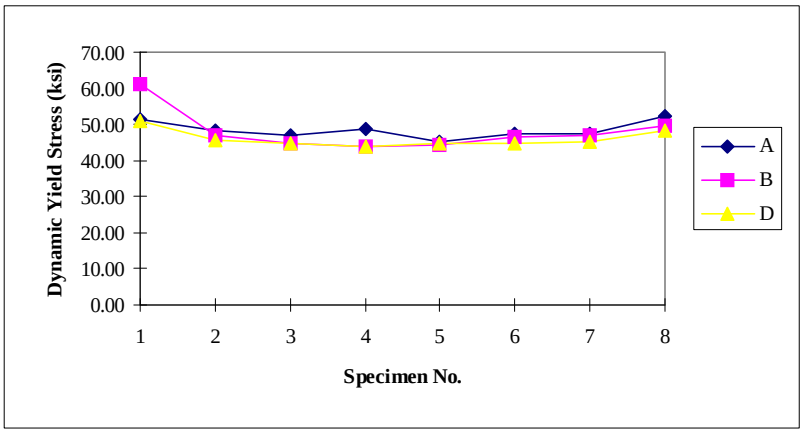

Fig 4.26 Comparison of the Dynamic Yield Stress for Specimen Types A, B and D (ksi)

Table 4.9 Comparison of the Dynamic Ultimate Stress for Specimen Types A, B and D (ksi)

$F_{u\text{-}dyn}$	Types		
Specimen No.	A	B	D
1	71.54	73.70	72.50
2	72.45	73.12	70.75
3	71.75	72.89	70.32
4	70.84	71.71	69.06
5	70.91	72.67	70.29
6	71.35	73.01	70.77
7	71.42	73.06	71.02
8	72.12	72.07	71.18
Average	71.55	72.78	70.74
STDEV	0.55	0.63	0.97

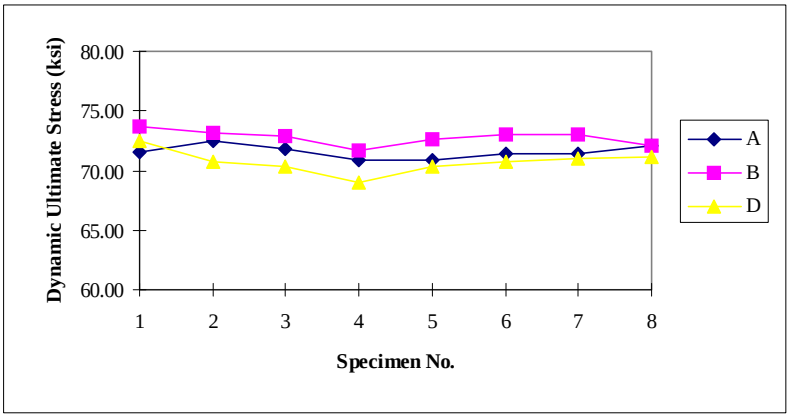

Fig 4.27 Comparison of the Dynamic Ultimate Stress for Specimen Types A, B and D (ksi)

Table 4.10 Comparison of the Static Yield Stress for Specimen Types A, C and E (ksi)

$F_{y\text{-static}}$	Types		
Specimen No.	A	C	E
1	47.10	48.92	60.55
2	44.76	44.76	60.80
3	44.13	43.22	59.65
4	42.38	43.35	60.13
5	42.43	43.65	61.26
6	43.98	43.72	62.00
7	44.18	44.59	62.45
8	49.40	56.70	59.62
Average	44.80	46.11	60.81
STDEV	2.37	4.66	1.04

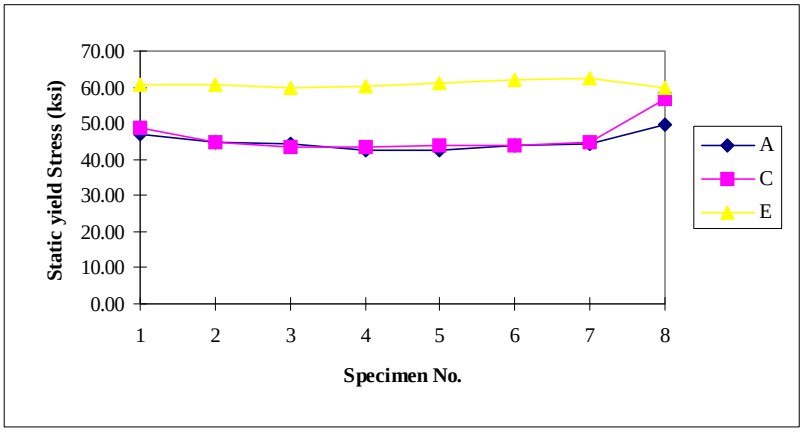

Fig 4.28 Comparison of the Static Yield Stress for Specimen Types A, C and E (ksi)

Table 4.11 Comparison of the Dynamic Yield Stress for Specimen Types A, C and E (ksi)

$F_{y\text{-}dyn}$	Types		
Specimen No.	A	C	E
1	51.19	52.08	63.52
2	48.20	47.82	63.81
3	47.12	46.58	62.65
4	48.67	45.99	63.18
5	44.97	46.84	64.24
6	47.50	47.73	65.17
7	47.51	48.36	65.71
8	52.34	59.59	62.26
Average	48.44	49.37	63.82
STDEV	2.34	4.53	1.19

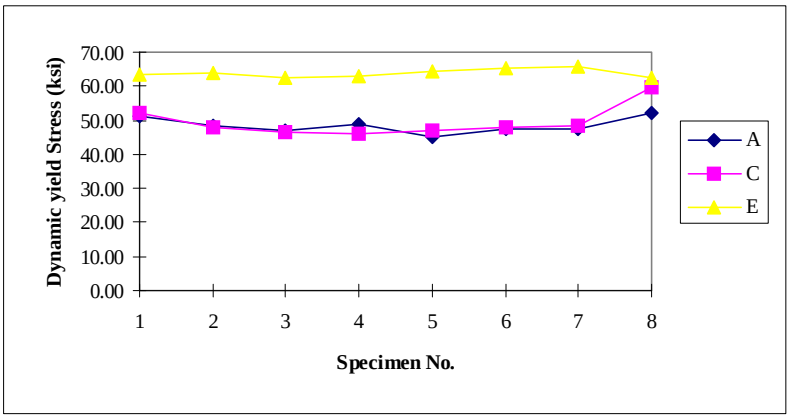

Fig 4.29 Comparison of the Dynamic Yield Stress for Specimen Types A, C and E (ksi)

Table 4.12 Comparison of the Dynamic Ultimate Stress for Specimen Types A, C and E (ksi)

$F_{u\text{-}dyn}$	Types		
Specimen No.	A	C	E
1	71.54	72.82	70.17
2	72.45	72.59	69.53
3	71.75	71.83	68.30
4	70.84	71.60	66.90
5	70.91	72.42	68.30
6	71.35	72.42	69.25
7	71.42	72.48	70.68
8	72.12	71.58	69.48
Average	71.55	72.22	69.08
STDEV	0.55	0.48	1.20

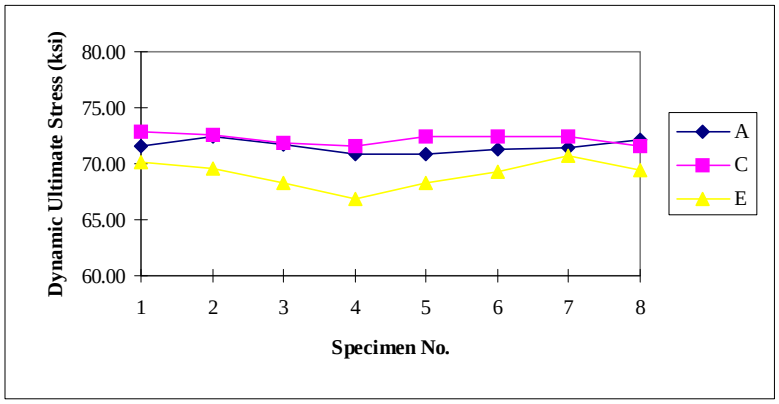

Fig 4.30 Comparison of the Dynamic Ultimate Stress for Specimen Types A, C and E (ksi)

Both Specimen Types B and D are 3 in long sub-length specimens along the rolling direction and through-thickness direction, respectively. The results

show comparable values in dynamic ultimate stress, static yield stress and dynamic yield stress values. The slightly lower yield and ultimate stress for Specimen Type D may suggest slightly lower strength in the through thickness direction compared to the rolling direction. These results also suggest that the 3 in long sub-length coupons can give reliable and repeatable results for the yield and ultimate stress measurement along both the rolling and through-thickness direction.

Specimen Types C and E are 7 in long specimens prepared using welded prolongations along the rolling and the through-thickness direction respectively. Specimen Type E showed much higher static yield stress than Specimen Types A and C. As noted earlier, the reason for this anomaly is not known. Based on this results, however, it is unclear if yield stress values can be accurately determined in the through-thickness direction using coupons constructed with welded prolongations.

Tables 4.13 through 4.15 give the tensile strength properties for all of the specimens. The trends for the tensile properties for all of the specimens are shown in Figures 4.31 through 4.33.

Table 4.13 Comparison of the Static Yield Stress for all Specimens (ksi)

$F_{y\text{-static}}$	Types				
Specimen No.	A	B	C	D	E
1	47.10	49.03	48.92	47.58	60.55
2	44.76	43.12	44.76	42.95	60.80
3	44.13	42.53	43.22	42.29	59.65
4	42.38	41.16	43.35	41.20	60.13
5	42.43	42.13	43.65	42.14	61.26
6	43.98	43.62	43.72	42.34	62.00
7	44.18	44.81	44.59	42.99	62.45
8	49.40	47.00	56.70	45.63	59.62
Average	44.80	44.18	46.11	43.39	60.81
STDEV	2.37	2.66	4.66	2.12	1.04

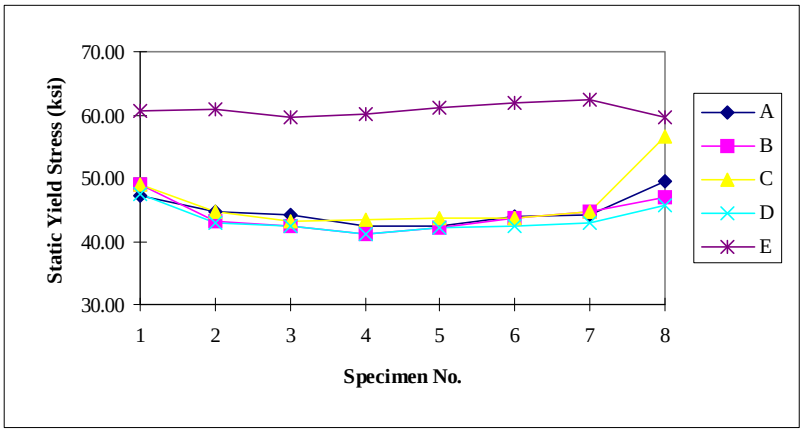

Fig 4.31 Comparison of the Static Yield Stress for all Specimens (ksi)

Table 4.14 Comparison of the Dynamic Yield Stress for all Specimens (ksi)

$F_{y\text{-}dyn}$	Types				
Specimen No.	A	B	C	D	E
1	51.19	61.20	52.08	50.73	63.52
2	48.20	47.16	47.82	45.64	63.81
3	47.12	44.84	46.58	44.54	62.65
4	48.67	44.00	45.99	43.76	63.18
5	44.97	44.43	46.84	44.58	64.24
6	47.50	46.56	47.73	44.55	65.17
7	47.51	47.03	48.36	45.37	65.71
8	52.34	49.67	59.59	48.28	62.26
Average	48.44	48.11	49.37	45.93	63.82
STDEV	2.34	5.60	4.53	2.37	1.19

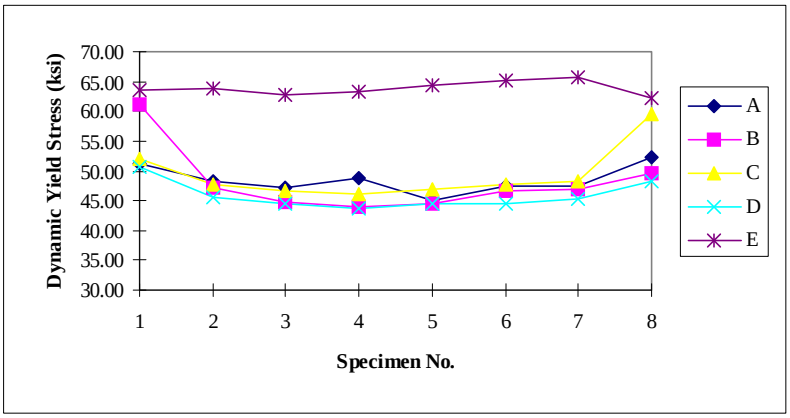

Fig 4.32 Comparison of the Dynamic Yield Stress for all Specimens (ksi)

Table 4.15 Comparison of the Dynamic Ultimate Stress for all specimens (ksi)

$F_{u\text{-}dyn}$	Types				
Specimen No.	A	B	C	D	E
1	71.54	73.70	72.82	72.50	70.17
2	72.45	73.12	72.59	70.75	69.53
3	71.75	72.89	71.83	70.32	68.30
4	70.84	71.71	71.60	69.06	66.90
5	70.91	72.67	72.42	70.29	68.30
6	71.35	73.01	72.42	70.77	69.25
7	71.42	73.06	72.48	71.02	70.68
8	72.12	72.07	71.58	71.18	69.48
Average	71.55	72.78	72.22	70.74	69.08
STDEV	0.55	0.63	0.48	0.97	1.20

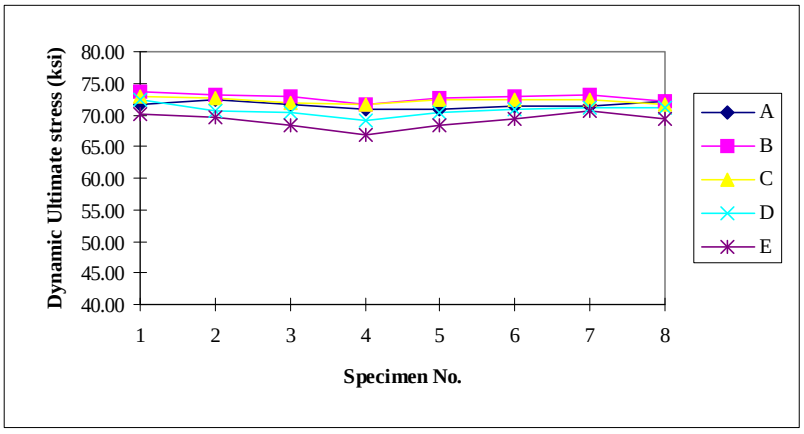

Fig 4.33 Comparison of the Dynamic Ultimate Stress for all Specimens (ksi)

From Tables 4.13 through 4.15 and previous comparisons, the data reveals that the yield and tensile stress for all specimen types are nearly identical, except for Specimen Type E, which showed much higher yield stress. Specimens in the

rolling direction (Types A, B and C) have a slightly larger dynamic ultimate stress than the specimens in the through-thickness direction (Types D and E).

For all the specimen types, the material near the center of the column flange showed somewhat lower strength than the material near the outer edges of the column flange. This phenomenon is more pronounced in the yield stress measurements than in the ultimate stress measurement.

As a final evaluation of the strength data, the dynamic ultimate stress ratio is examined. The dynamic ultimate strength ratio ($F_{u\text{-}dyn}$ ratio), can be written as:

$$F_{u\text{-}dyn\ Type1/Type2}\ \text{ratio} = F_{u\text{-}dyn\ Type\ 1} / F_{u\text{-}dyn\ Type\ 2}$$

Each of the $F_{u\text{-}dyn}$ ratios is plotted in Figures 4.34 through 4.38. In Figure 4.34**,** the dynamic ultimate strength of Type A ($F_{u\text{-}dyn\ TypeA}$) was used as the denominator in order to compare all of the other specimens, with respect to the Type A specimens. This data suggests that the through thickness ultimate stress for this material was on the order of 95 to 98 percent of the rolling direction value.

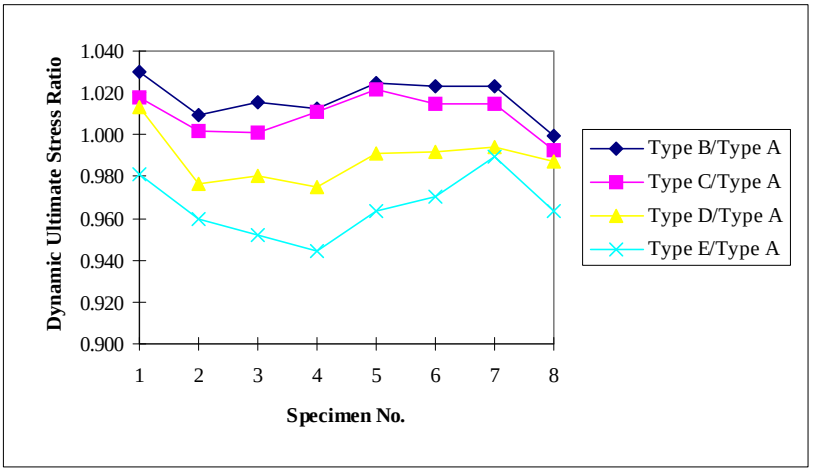

Fig 4.34. $F_{u\text{-}dyn}$ Ratio for Specimen Types B, C, D and E, with Respect to Type A Specimens.

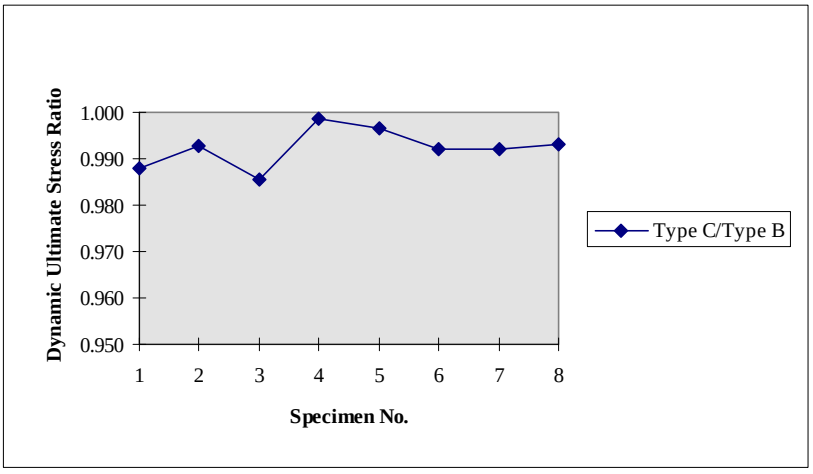

Fig 4.35 $F_{u\text{-}dyn}$ Ratio for Type C Specimens, with Respect to Type B Specimens

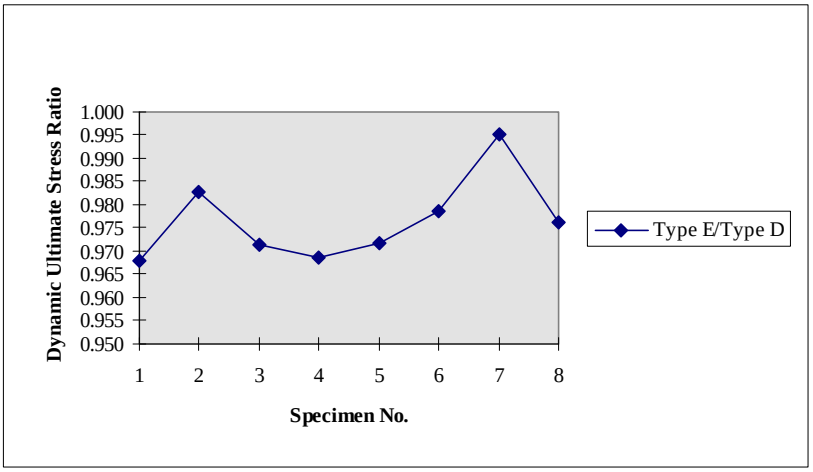

Fig 4.36 $F_{u\text{-}dyn}$ Ratio for Type E Specimens, with Respect to Type D Specimens

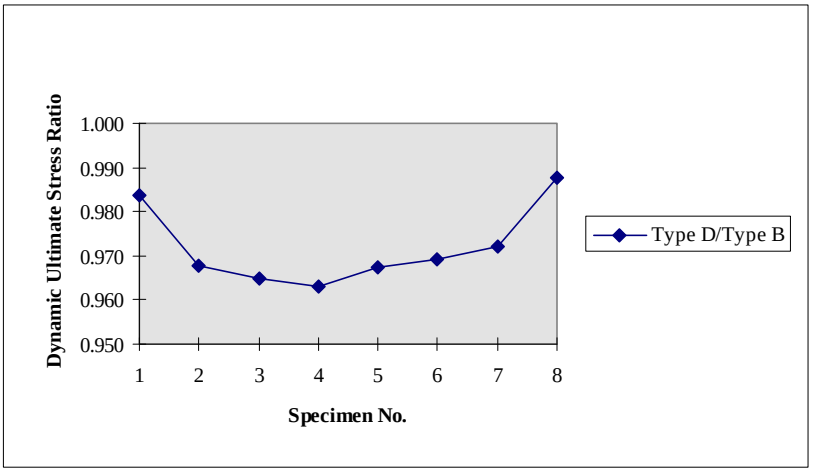

Fig 4.37 $F_{u\text{-}dyn}$ Ratio for Type D Specimens, with Respect to Type B Specimens

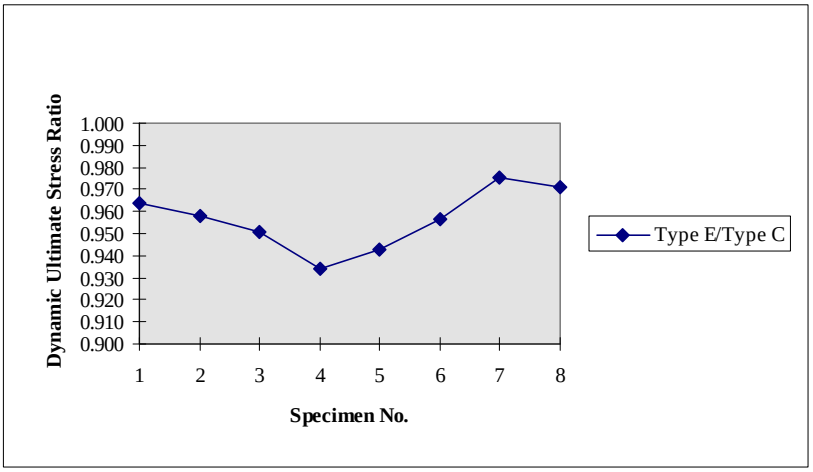

Fig 4.38 $F_{u\text{-}dyn}$ Ratio for Specimen Type E with Respect to Type C Specimens

4.3 Elongation and Reduction in Area Results

4.3.1 Comparison of Specimens in the Rolling Direction

The ductility properties in the rolling direction, measured by the percent elongation (%EL) and percent reduction in area (%RA) for Types A, B and C specimens are given in Table 4.16 and Table 4.17. The trends for the ductility properties are shown in Figures 4.39 Through 4.40, while the results for the individual specimens are plotted in Figures 4.41 through 4.46.

Table 4.16 Comparison of the %RA for Specimen Types A, B and C

%RA	Types		
Specimen No.	A	B	C
1	64.00	68.22	69.09
2	62.26	62.60	61.37
3	63.67	62.74	63.81
4	63.47	62.21	62.99
5	61.19	64.57	62.69
6	64.61	64.52	64.38
7	63.14	62.02	65.15
8	69.58	68.61	68.22
Average	63.99	64.44	64.71
STDEV	2.49	2.64	2.69

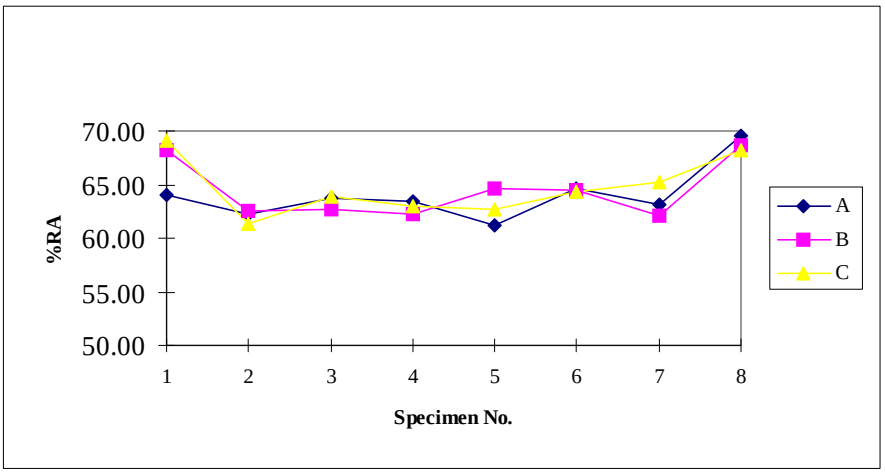

Fig 4.39 Comparison of the %RA for Specimen Types A, B and C

Table 4.17 Comparison of the %EL for Specimen Types A, Band C

%EL	Types		
Specimen No.	A	B	C
1	23.71	32.74	34.82
2	22.91	29.39	33.71
3	22.53	31.87	33.21
4	22.56	30.35	33.57
5	23.07	30.65	34.42
6	20.95	31.36	33.59
7	22.51	31.47	34.58
8	21.35	32.74	36.29
Average	22.45	31.32	34.27
STDEV	0.90	1.16	0.99

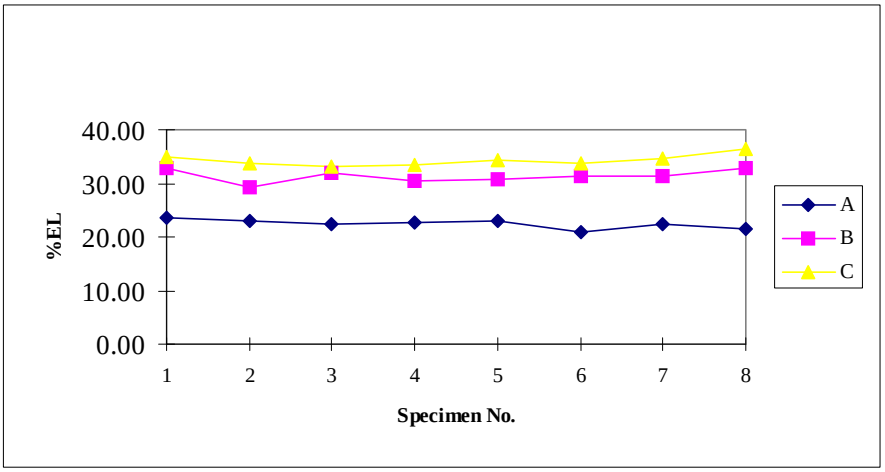

Fig 4.40 Comparison of the %EL for Specimen Types A, Band C

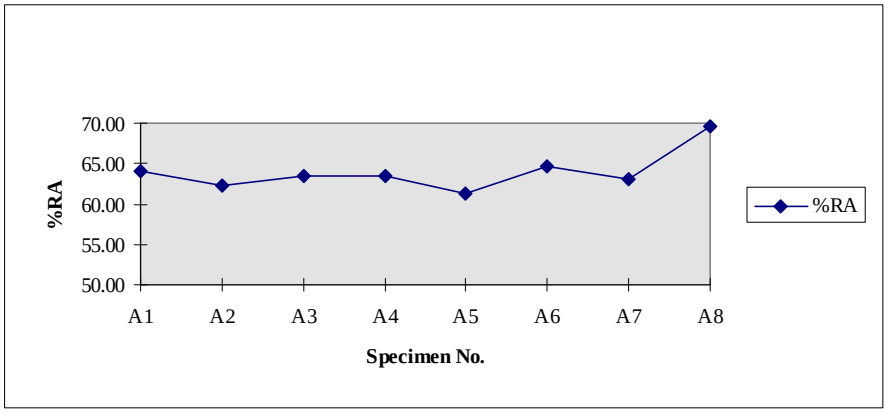

Fig 4.41 The %RA for Type A Specimens

Fig 4.42 The %RA for Type B Specimens

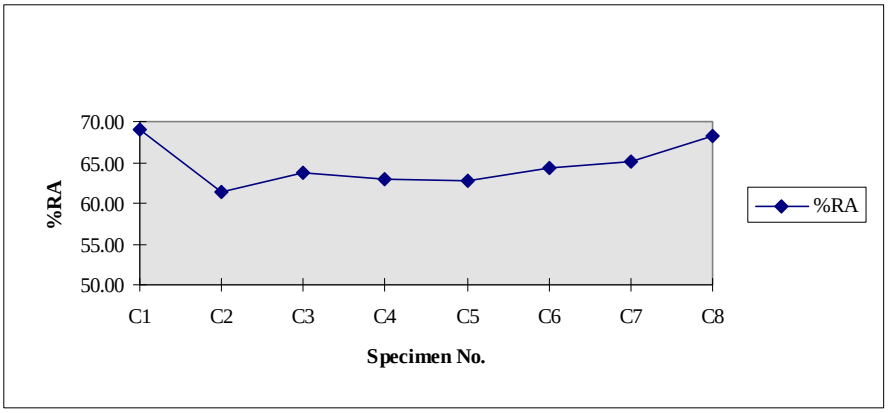

Fig 4.43 The %RA for Type C Specimens

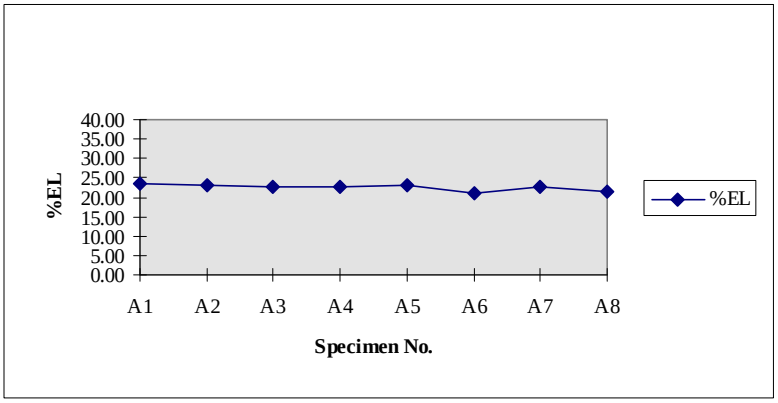

Fig 4.44 The %EL for Type A Specimens

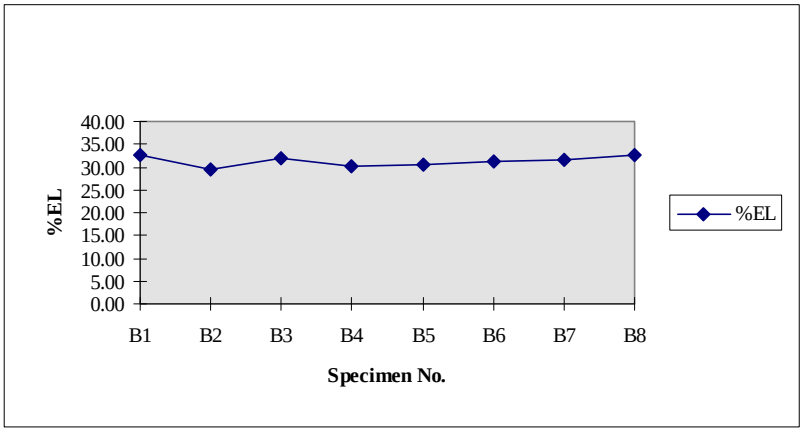

Fig 4.45 The %EL for Type B Specimens

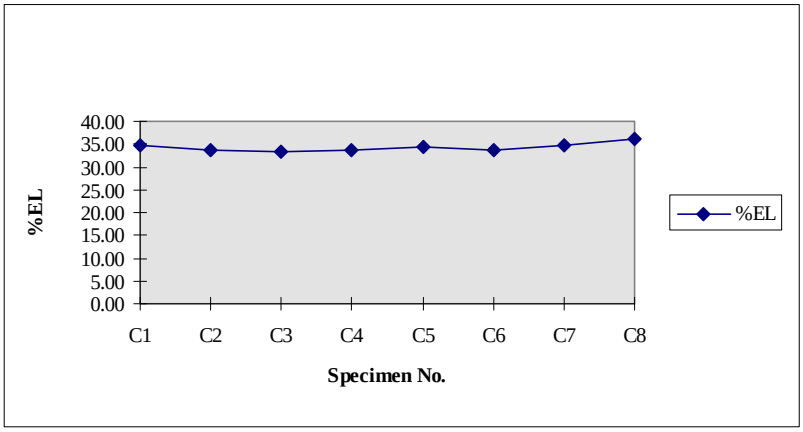

Fig 4.46 The %EL for Type C Specimens

The data indicates that the three coupon types in the rolling direction provided very similar reduction in area values. The average reduction in area values varied in the very small range of 64% to 65% for the three coupon types, as shown in Table 4.16. The variability in reduction in area measurements, as indicated by the standard deviation in Table 4.16, was also very similar for the three coupon types.

The percent elongation measurements, on the other hand, showed much larger differences among the three coupon types in the rolling direction. The average percent elongation for coupon Types A, B and C were 22.5, 31.3 and 34.3, respectively. For Specimen Type A, the necked down region of the coupon usually occurred outside of the 2 inch gage marks, whereas the Types B and C, it typically occurred within the gage marks. Thus, the differences in percent elongation measurements appears to reflect the different necking location with respect to the gage marks.

4.3.2 Comparison of Specimens in the Through-Thickness Direction

The ductility properties in the through-thickness direction, measured by the percent elongation (%EL) and the percent reduction in area (%RA) for the Type D and Type E specimens, are given in Tables 4.18 and 4.19**.** The ductility properties for Type A specimens are also shown, as a reference. The trends for the ductility properties are shown in Figures 4.47 through 4.48, whereas the results for individual specimens are shown in Figures 4.49 through 4.52.

Table 4.18 Comparison of the %RA for Specimen Types A, D and E

%RA	Types		
Specimen No.	A	D	E
1	64.00	54.31	55.64
2	62.26	22.87	23.92
3	63.67	23.52	13.54
4	63.47	21.69	10.89
5	61.19	22.52	13.99
6	64.61	16.40	17.45
7	63.14	17.03	23.08
8	69.58	44.56	21.11
Average	63.99	27.86	22.45
STDEV	2.49	13.82	14.22

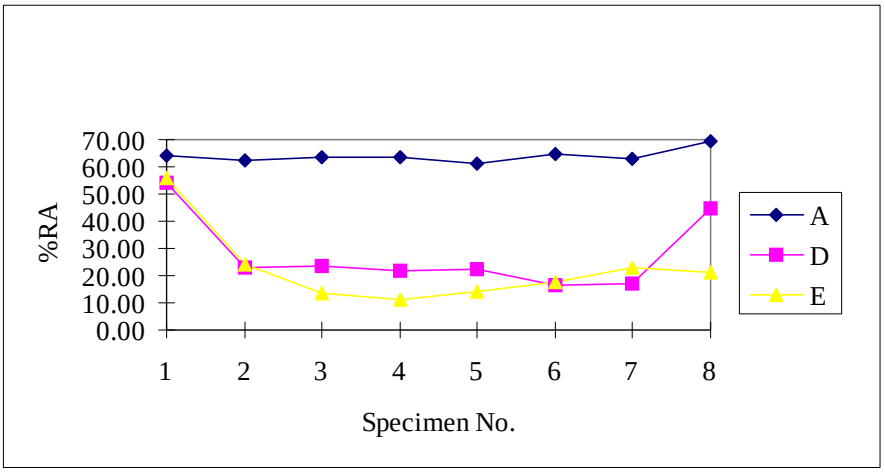

Fig 4.47 Comparison of the %RA for Specimen Types A, D and E

Table 4.19 Comparison of the %EL for Specimen Types A, D and E

%EL	Types		
Specimen No	A	D	E
1	23.71	27.41	29.07
2	22.91	16.56	16.95
3	22.53	16.29	13.61
4	22.56	15.51	9.24
5	23.07	16.20	13.17
6	20.95	15.40	12.90
7	22.51	14.32	18.20
8	21.35	25.68	12.43
Average	22.45	18.42	15.70
STDEV	0.90	5.08	6.07

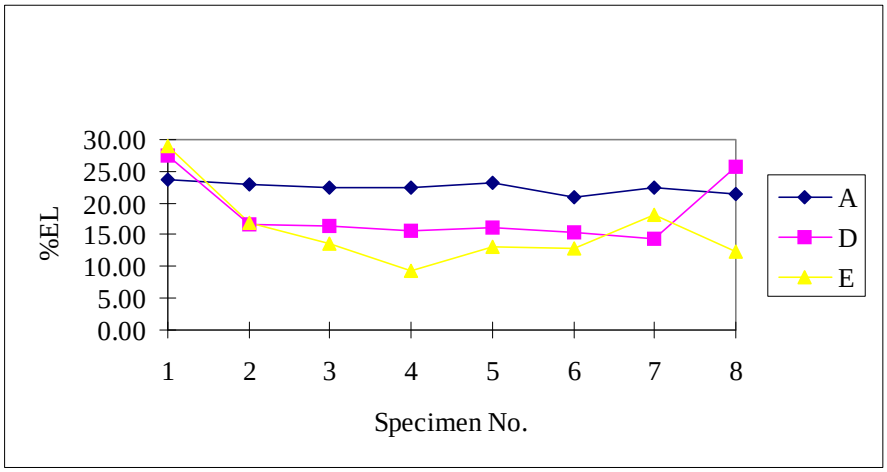

Fig 4.48 Comparison of the %EL for Specimen Types A, D and E

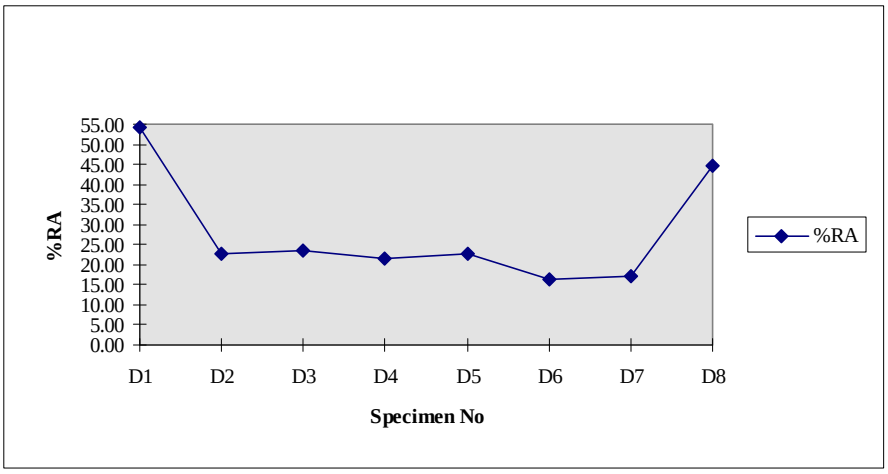

Fig 4.49 Comparison of the %RA for Type D Specimens

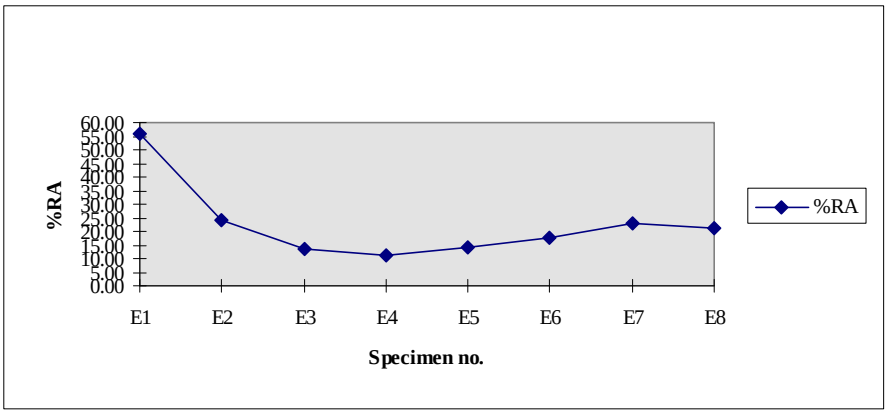

Fig 4.50 Comparison of the %RA for Type E Specimens

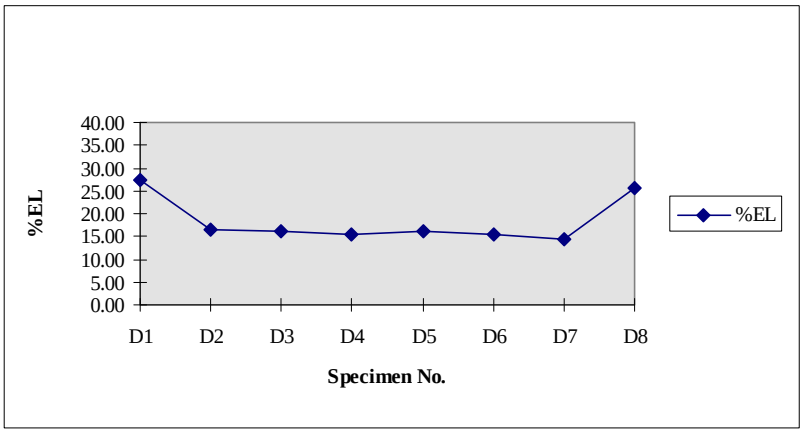

Fig 4.51 Comparison of the %EL for Type D Specimens

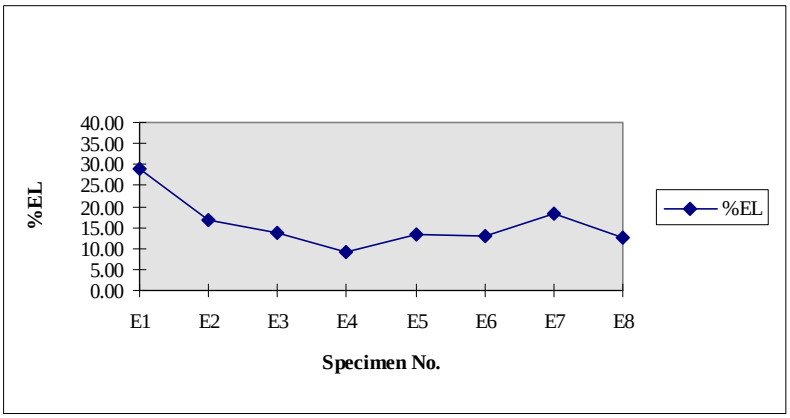

Fig 4.52 Comparison of the %EL for Type E Specimens

Several interesting observations can be made with respect to the reduction in area results for the through-thickness coupons.(Table 4.18) First, both coupon

types in the through-thickness direction (Types D, E) showed very large variability in the results. For example, for specimen Type D, the reduction in area varied from 16.4% to 54.3% for the eight specimens. For specimen Type E, reduction in area varied from about 10.9% to 55.6% for the eight specimens. This variability is reflected in the large standard deviation values for Specimen Type D and E in Table 4.18. Compare this to the much smaller standard deviation for Specimen Type A in the rolling direction. For Specimen Type A, the coefficient of variation (standard deviation divided by mean) is only about 4 percent. For Specimen Types D and E in the through-thickness direction, the coefficient of variation are 50% and 63%, respectively.

The data in Table 4.18 also indicate that the two different types of through-thickness specimens gave somewhat different reduction in area values. Specimen Type E, with welded prolongations, gave an average reduction in area of 22.5%, compared to 27.9% for Specimen Type D. The smaller reduction in area values in the Type E specimens may reflect an adverse effect of the welding. However, considering the large variability in results, no clear conclusions can be drawn from the differences between Specimen Types D and E.

The final conclusion that can be drawn from the data in Table 4.18 is that the reduction of areas for the through-thickness coupons (Types D and E) were dramatically less than for the rolling direction coupon (Type A). In the through-thickness direction, the percent reduction in area was on the order of one-third to one-half the value measured in the rolling direction.

Results for the percent elongation measurements (Table 4.19) also show much larger variations in the through-thickness direction than in the rolling direction. The two different coupon Types in the through-thickness direction

show somewhat different average percent elongation, with the similar values occurring for the coupons with welded prolongations. Finally, the data in Table 4.19 indicate smaller elongation values in the through-thickness direction compared with the rolling direction. The differences, however, are not nearly as large as observed in the reduction in area measurements. As discussed earlier, the percent elongation measurements are significantly affected by the location of the necked down region with respect to the gage marks.

4.3.3 Comparison of All Specimens

A comparison of the ductility properties between the specimens in the rolling direction (Types B and C) and the specimens in the through-thickness direction (Types D and E) are given in Tables 4.20 through 4.23**.** The trends for the ductility properties are graphically depicted in Figures 4.53 through 4.55**.** Tables 4.24 through 4.25 give the ductility properties of all of the specimens, while the trends of the ductility properties for all of the specimens are shown in Figures 4.57 through 4.58.

Table 4.20 Comparison of the %RA for Specimen Types A, B and D

%RA	Types		
Specimen No.	A	B	D
1	64.00	68.22	54.31
2	62.26	62.60	22.87
3	63.67	62.74	23.52
4	63.47	62.21	21.69
5	61.19	64.57	22.52
6	64.61	64.52	16.40
7	63.14	62.02	17.03
8	69.58	68.61	44.56
Average	63.99	64.44	27.86
STDEV	2.49	2.64	13.82

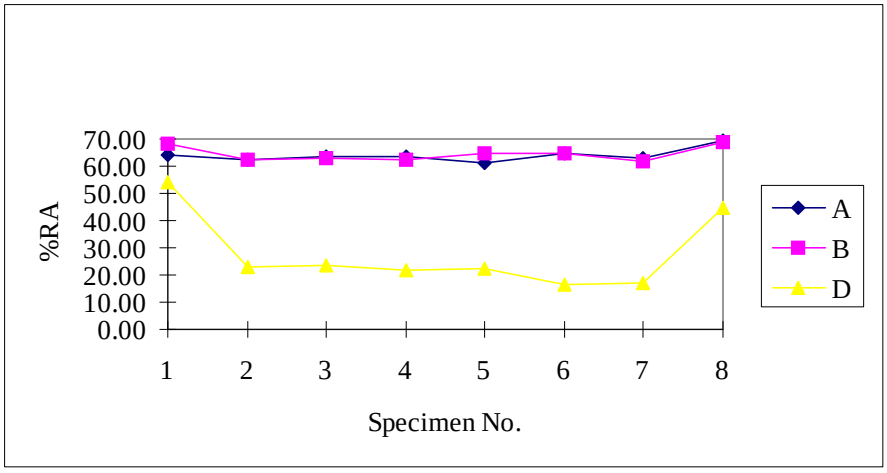

Fig 4.53 Comparison of the %RA for Specimen Types A, B and D

Table 4.21 Comparison of the EL% for Specimen Types A, Band D

%EL	Types		
Specimen No.	A	B	D
1	23.71	32.74	27.41
2	22.91	29.39	16.56
3	22.53	31.87	16.29
4	22.56	30.35	15.51
5	23.07	30.65	16.20
6	20.95	31.36	15.40
7	22.51	31.47	14.32
8	21.35	32.74	25.68
Average	22.45	31.32	18.42
STDEV	0.90	1.16	5.08

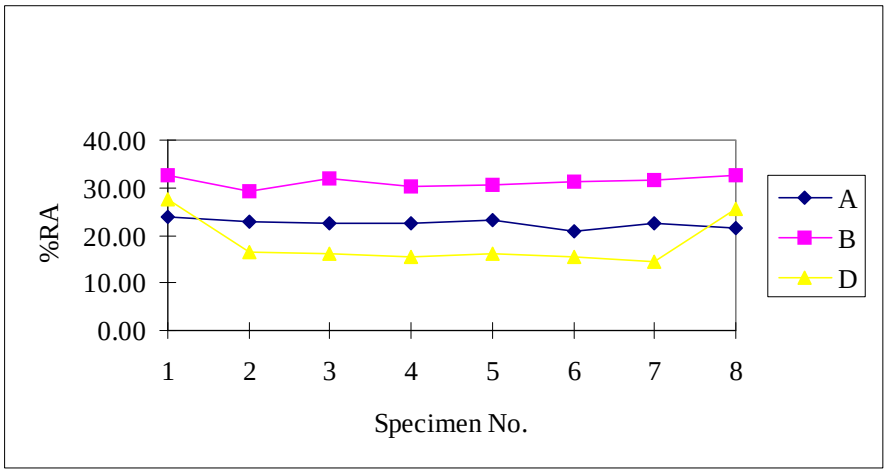

Fig 4.54 Comparison of the %RA for Specimen Types A, B and D

Table 4.22 Comparison of the %RA for Specimen Types A, C and E

%RA	Types		
Specimen No.	A	C	E
1	64.00	69.09	55.64
2	62.26	61.37	23.92
3	63.67	63.81	13.54
4	63.47	62.99	10.89
5	61.19	62.69	13.99
6	64.61	64.38	17.45
7	63.14	65.15	23.08
8	69.58	68.22	21.11
Average	63.99	64.71	22.45
STDEV	2.49	2.69	14.22

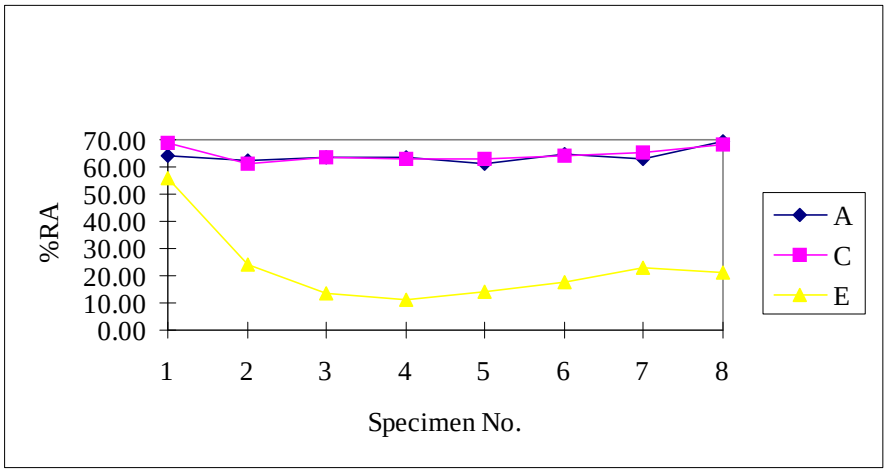

Fig 4.55 Comparison of the %RA for Specimen Types A, C and E

Table 4.23 Comparison of the %EL for Specimen Types A, C and E

EL%	Types		
Specimen No.	A	C	E
1	23.71	34.82	29.07
2	22.91	33.71	16.95
3	22.53	33.21	13.61
4	22.56	33.57	9.24
5	23.07	34.42	13.17
6	20.95	33.59	12.90
7	22.51	34.58	18.20
8	21.35	36.29	12.43
Average	22.45	34.27	15.70
STDEV	0.90	0.99	6.07

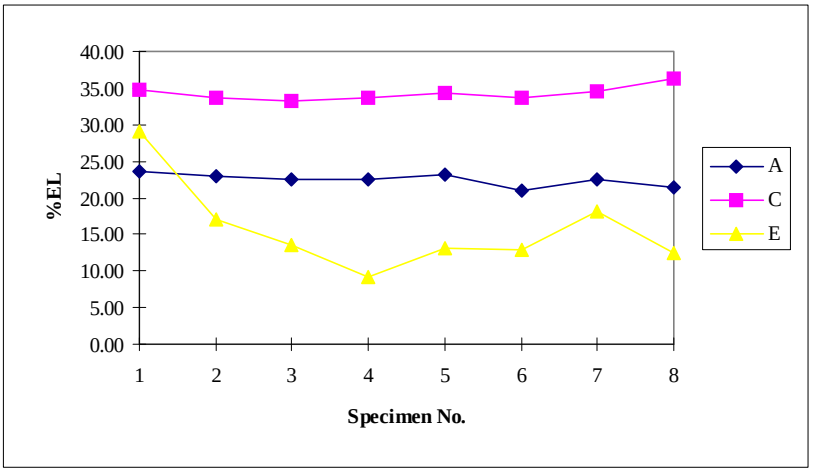

Figure 4.56 Comparison of the %EL for Specimen Types A, C and E

Results for the reduction in area measurements (Tables 4.20, 4.22) showed many conclusive points for the difference between specimens in the rolling and through-thickness direction.

The data in Table 4.20 indicate that the two sub-length specimens (Types B, D) taken along the rolling direction and through-thickness direction had large

differences in the reduction in area measurements. Specimen Type D, taken along the through-thickness direction, gave a much smaller average reduction in area value of 27.9%, compared to 64.4% for Specimen Type B. The smaller reduction in area values in the Type D specimens reflect the significantly reduced ductility in the through-thickness direction. The variability is reflected in the standard deviation values, which are 13.8%, 2.5% and 2.6% for Specimen Types D, A, and B, respectively. Also, the coefficient of variation for Specimen Type D is as large as 50%. For Specimen Types A and B in the rolling direction, the coefficient of variation are only 4% for both.

From the data shown in Table 4.22, several trends can be summarized. Specimen Types C and E are specimens with welded prolongations along the rolling and through-thickness direction, respectively. Again, the specimens taken along the through-thickness direction (Specimen Type E) showed much smaller average reduction in area values about 22.5%, compared to 64.7% for Specimen Type C. Also, the coefficient of variations are 63%, 4% and 4%, respectively.

In terms of the percent elongation measurements (Tables 4.21, 4.23), however the differences between the specimens taken along the through-thickness direction (Types D, E) and the specimens taken along the rolling direction were not as large as in the reduction in area measurements. The difference was about 13% between Types B, D and about 19% between Types C, E. Also, the standard deviation values observed in the percent elongation measurements were smaller than in the reduction in area measurements.

Table 4.24 Comparison of the %RA for all of the Specimens

%RA	Types				
Specimen No.	A	B	C	D	E
1	64.00	68.22	69.09	54.31	55.64
2	62.26	62.60	61.37	22.87	23.92
3	63.67	62.74	63.81	23.52	13.54
4	63.47	62.21	62.99	21.69	10.89
5	61.19	64.57	62.69	22.52	13.99
6	64.61	64.52	64.38	16.40	17.45
7	63.14	62.02	65.15	17.03	23.08
8	69.58	68.61	68.22	44.56	21.11
Average	63.99	64.44	64.71	27.86	22.45
STDEV	2.49	2.64	2.69	13.82	14.22

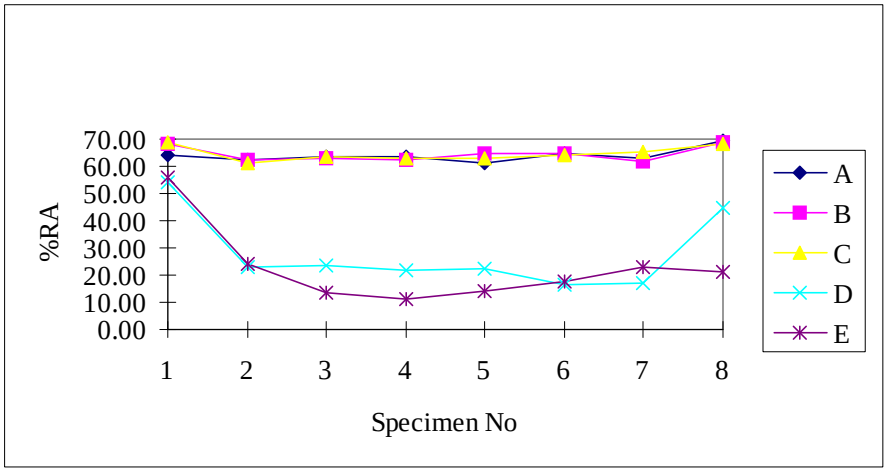

Fig 4.57 Comparison of the %RA for all of the Specimens

Table 4.25 Comparison of the %EL for all of the Specimens

%EL	Types				
Specimen No.	A	B	C	D	E
1	23.71	32.74	34.82	27.41	29.07
2	22.91	29.39	33.71	16.56	16.95
3	22.53	31.87	33.21	16.29	13.61
4	22.56	30.35	33.57	15.51	9.24
5	23.07	30.65	34.42	16.20	13.17
6	20.95	31.36	33.59	15.40	12.90
7	22.51	31.47	34.58	14.32	18.20
8	21.35	32.74	36.29	25.68	12.43
Average	22.45	31.32	34.27	18.42	15.70
STDEV	0.90	1.16	0.99	5.08	6.07

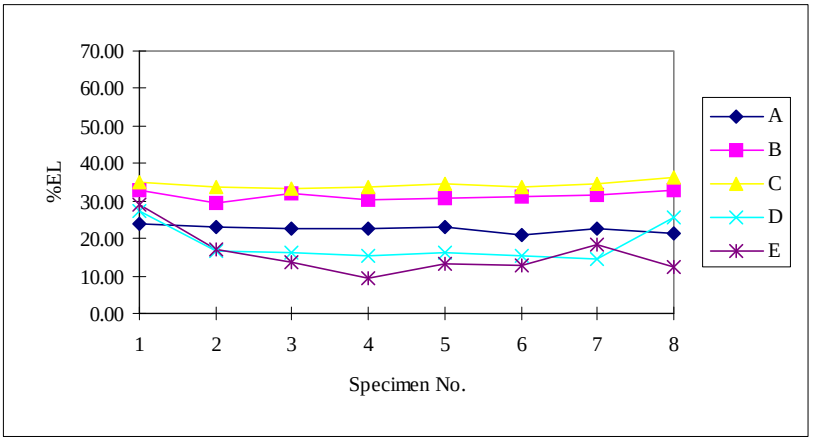

Fig 4.58 Comparison of the %EL for all of the Specimens

The data in Figs 4.57 and 4.58 indicate that the material near the edges of the column flange gave higher values in reduction in area measurements and

percent elongation measurements. This trend is similar to that observed in the strength level measurements as discussed in Section 4.2.

It is noted that as the tensile strength increased, the reduction in area values and percent elongation values also increased. This trend agrees with other research results found in the literature search. [7]

As a final evaluation of ductility data, The percent reduction in area ratio is examined: The percent reduction in area ratio is:

$$\%RA_{Type1/Type2}\ \text{Ratio} = \%RA_{Type1}/\%RA_{Type\ 2}$$

Each of the %RA ratios is plotted in Figures 4.66 through 4.70. In Figure 4.66, the percent reduction in area value for Type A specimens ($\%RA_{TypeA}$) was used as the denominator in order to compare Types B, C, D and E specimens, with respect to Type A specimens.

The data showed that Specimen Types B and C have a very consistent correlation with respect to Type A specimens, whereas Type D and E specimens have more variability. The trends are similar with what have been discussed in the tensile strength measurements (Section 4.2) that the outer edges of the column flange showed less difference in reduction in area values and percent elongation values than the center of the column flange. This data also shows the dramatic difference in reduction in area values in the through-thickness and rolling direction.

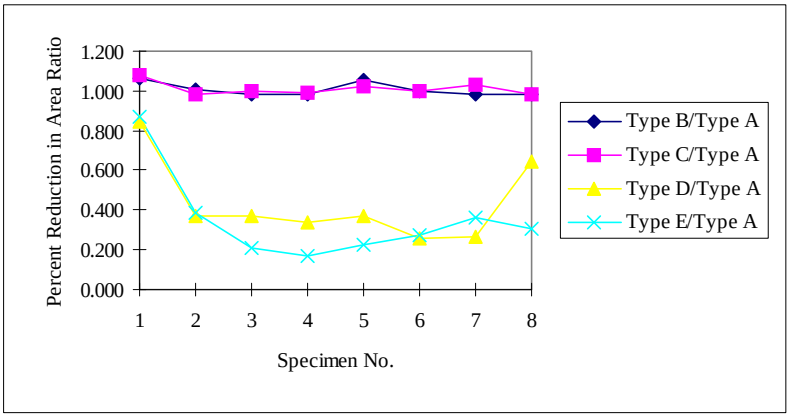

Fig 4.59 The %RA Ratio for Specimen Types B, C, D and E with Respect to Type A Specimens

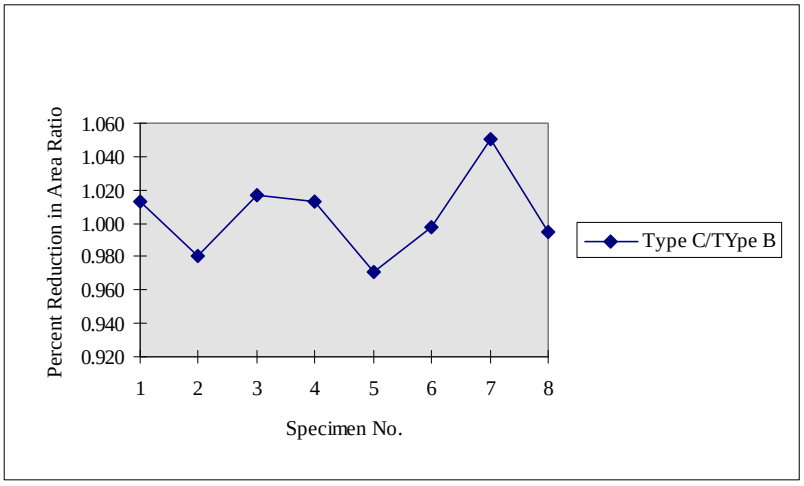

Fig 4.60 The %RA Ratio for Type C Specimens, with Respect to Type B Specimens

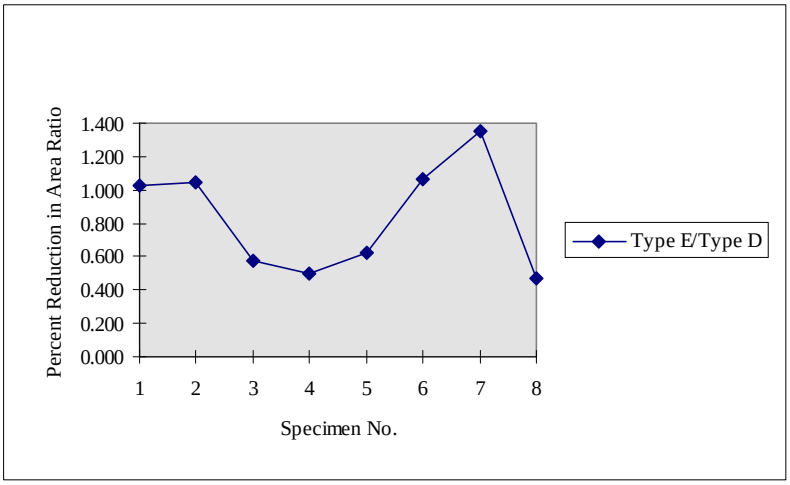

Fig 4.61 The %RA Ratio for Type E Specimens, with Respect to Type D Specimens

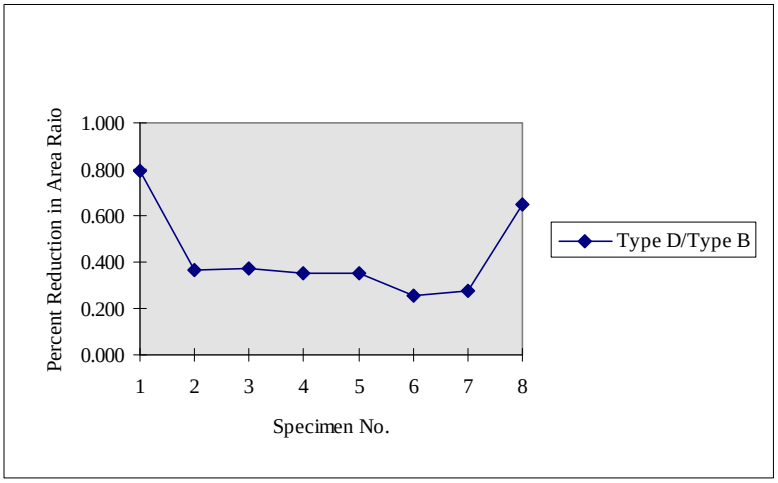

Fig 4.62 The %RA Ratio for Type D Specimens, with Respect to Type B Specimens

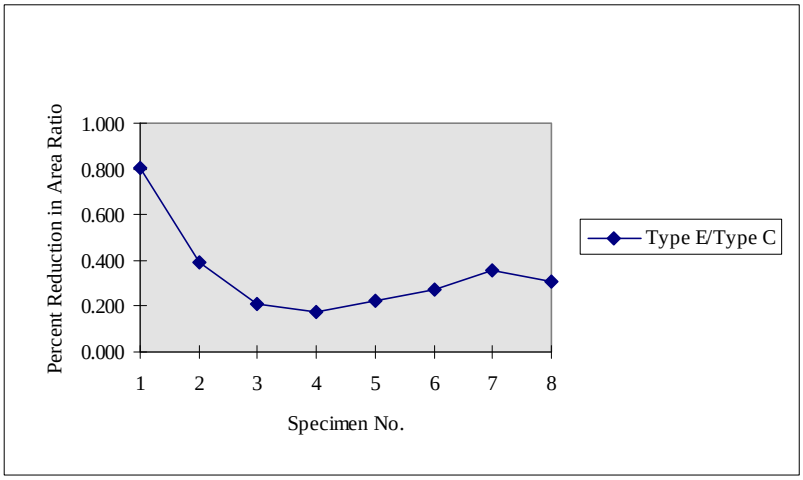

Fig 4.63 The %RA Ratio for Type E Specimens, with Respect to Type C Specimens

4.3.4 Appearance of Fractured Specimens

Figures 4.59 through 4.63 show the final fractured coupons for all of the specimen types. It is noted that Coupon D6 fractured near the coupon shoulder end and Coupon E4 fractured close to the welding. Consequently, test results for these two coupons might have been affected. Otherwise, all other coupons fractured away from the welds and coupon shoulders, and should have provided valid results.

The significantly larger reduction of areas in the rolling direction coupons compared to the through-thickness coupons is apparent in the photos.

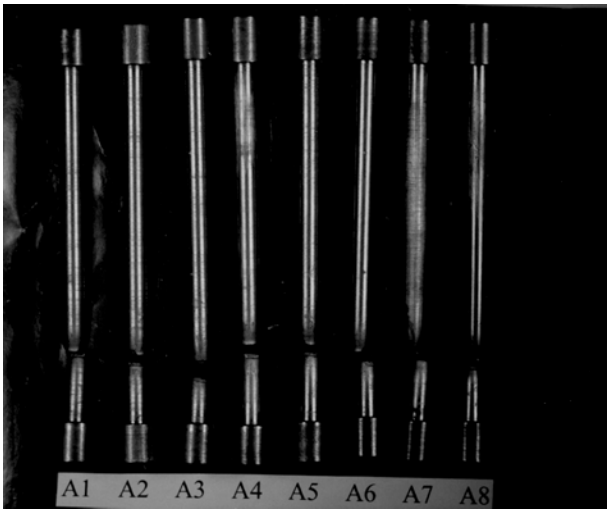

Fig 4.64 Type A Specimen Fractures

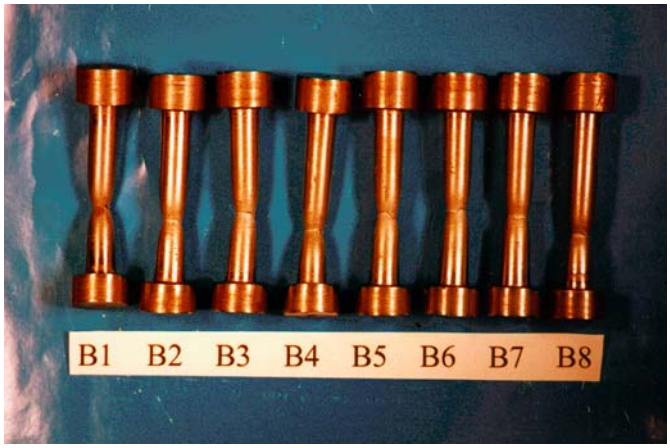

Fig 4.65 Type B Specimen Fractures

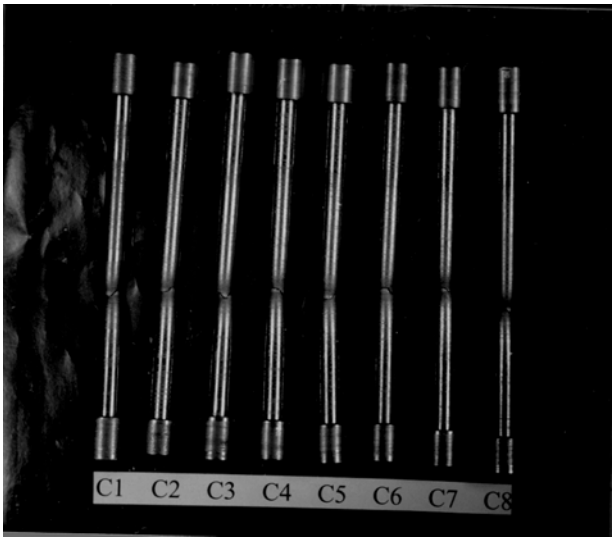

Fig 4.66 Type C Specimen Fractures

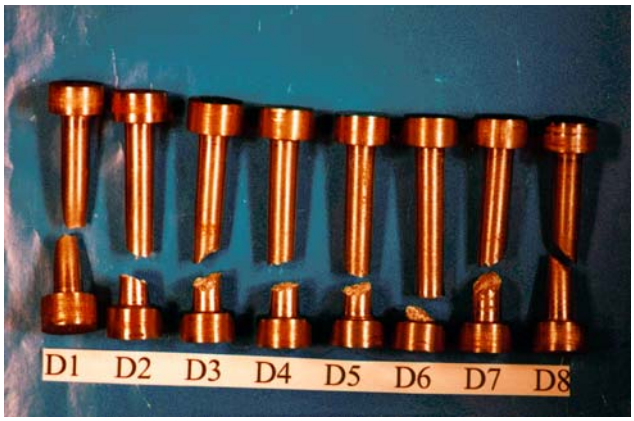

Fig 4.67 Type D Specimen Fractures

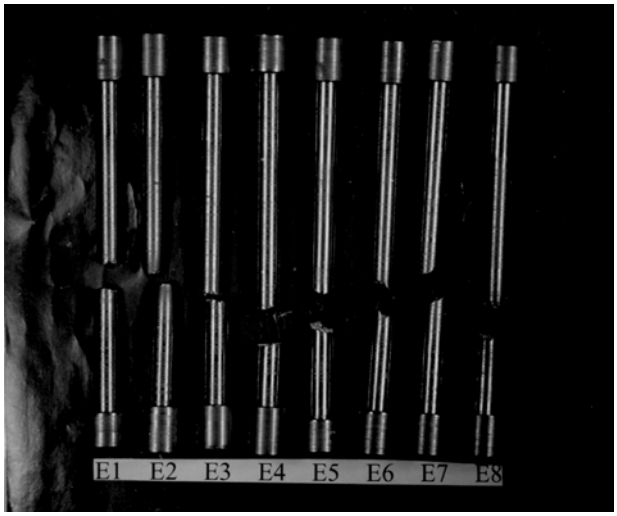

Fig 4.68 Type E Specimen Fractures

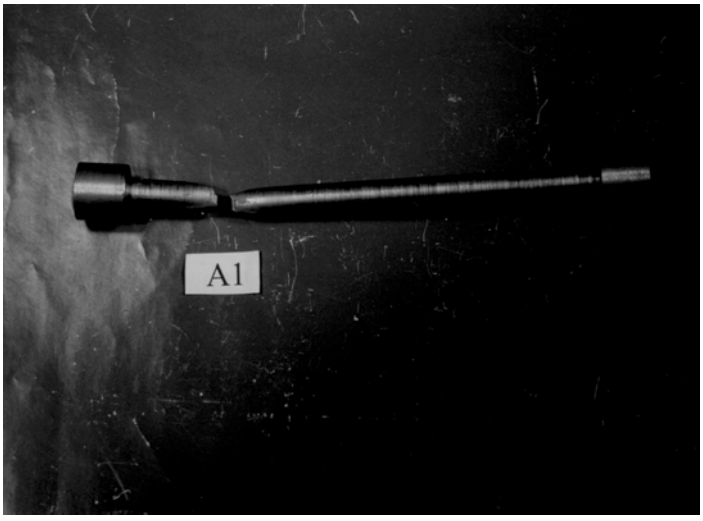

Fig 4.69 An A1 Specimen Fracture

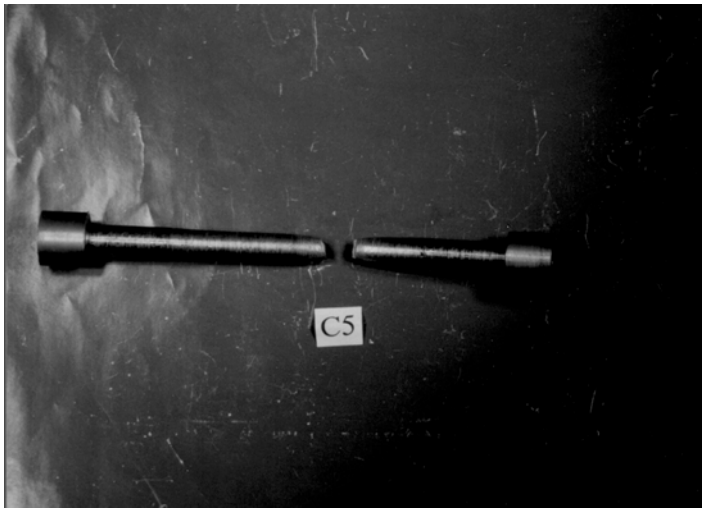

Fig 4.70 A C5 Specimen Fracture

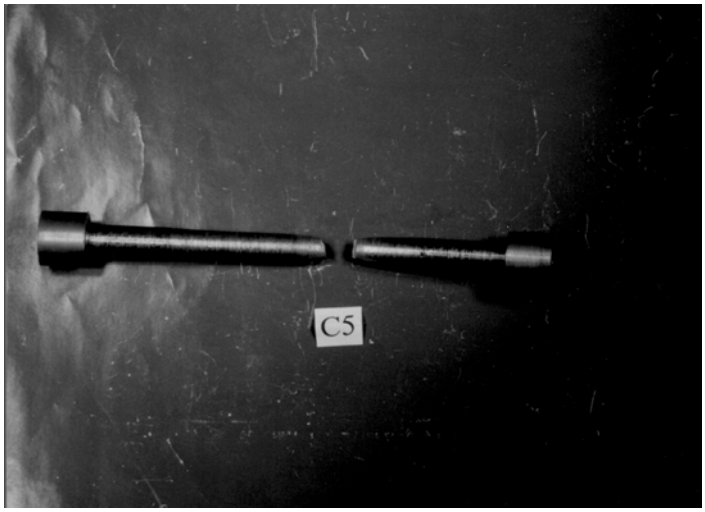

Fig 4.70 A C5 Specimen Fracture

4.4 Chemical Analysis

The data presented in the previuos sections indicate that material samples taken near the outer edges of the column flange generally showed higher yield stresses and higher reduction in area values than samples near the center portion of the column flange width. To determine if these differences were related to differences in chemical composition, samples of four coupons of Type D specimens were sent to a commercial testing laboratory for chemical analysis. The results are shown in Table 4.26. Specimens D1 and D8 were taken near the outer edges of the flange, whereas D4 and D5 were taken near mid-width of the flange. The results show nearly identical chemical compositions among the four samples. Consequently, the differences in yield stress and reduction in area values across the width of the flange did not result from differences in chemical

composition. The different mechanical properties near the outer edges of the column flanges may be due to differences in microstructure, perhaps related to different cooling rates experiened at various locations of the column cross-section during manufacturing the shape.

Table 4.26 The Chemical Component for Specimens D1, D4, D5 and D8Fig 4.36 $F_{u\text{-}dyn}$ Ratio for Type E Specimens, with Respect to Type D Specimens

Type D Specimens	Chemical Analysis			
Component	D1	D4	D5	D8
C	0.1600	0.1600	0.1600	0.1600
S	0.0220	0.0230	0.0220	0.0210
Mn	1.1200	1.1300	1.1200	1.1100
P	0.0190	0.0190	0.0190	0.0180
Si	0.3300	0.3300	0.3300	0.3300
Cr	0.0200	0.0200	0.0200	0.0200
Mo	0.0030	0.0030	0.0030	0.0030
Ni	0.0200	0.0200	0.0200	0.0200
Cu	0.0500	0.0500	0.0500	0.0500
V	0.0010	0.0010	0.0010	0.0010
Cb	0.0390	0.0400	0.0390	0.0380
Ti	0.0010	0.0010	0.0010	0.0010
Al	0.0170	0.0170	0.0170	0.0170
Sn	0.0030	0.0030	0.0030	0.0030
B	0.0002	0.0002	0.0002	0.0002
N	0.0053	0.0052	0.0054	0.0054
Fe	Balance	Balance	Balance	Balance

CHAPTER 5

CONCLUSIONS

This thesis has presented a comparison between 7-in (177.8-mm) long modified standard tensile coupons in the rolling direction, 3-in (76.2-mm) long sub-length tensile coupons in both the rolling and the through-thickness direction and 7-in (177.8-mm) long tensile coupons that were prepared using welded prolongations in both the rolling and the through-thickness direction. The experiments were performed to evaluate tension specimen design, variability in mechanical properties along the flange width, and differences in strength and ductility measurements among different coupon types. Much of the work included in this thesis is concerned with the design and the preparation of test specimens that will provide meaningful and repeatable results for the measurement of through-thickness tensile properties. All tests were conducted on a single sample of column flange material, taken from a W14×426 section of A572 Gr. 50 Steel.

Primary conclusions of this study can be summarized as follows:

- The two different methods of preparing through-thickness tension coupons (sub-length coupon and welded coupon) provided very consistent measurements of dynamic ultimate stress. Thus, it appears that dynamic ultimate stress can be reliably measured by either coupon type.

- The two methods of preparing through-thickness tension coupons gave reasonably consistent measurements of the percent reduction of area. The welded coupon gave slightly lower percent reduction of area values than the sub-length coupons. This may have reflected the influence of the welding, or may have simply reflected the large variability in the reduction of area measurements in the through-thickness direction. Nonetheless, the data suggests that reliable percent reduction of area measurements can be obtained from either coupon type.

- Measured yield stress values, both static and dynamic, differed significantly for the two different types of through-thickness tension coupons. The coupons made with welded prolongations showed significantly higher yield stress values than the sub-length coupons. The reason for this difference is not known. No such difference was observed between the welded coupons and sub-length coupons in the rolling direction. Based on these results, it is unclear if reliable yield stress measurements can be obtained in the through-thickness direction using welded coupons. Additional research is needed on this topic.

- The percent elongation measurements were rather inconsistent among all the coupon types tested, both in the rolling and through-thickness directions. These differences appeared to results from the fact that the necking and fracture locations in the coupons often did not fall between the 2 inch initial gage marks.

- The dynamic ultimate stress of the through-thickness coupons was, on average, 95 to 98 percent of the dynamic ultimate stress of the rolling direction coupons. Thus, it appears that for the particular material sampled in

this program, the ultimate stress was nearly the same in the rolling and through-thickness directions, with perhaps only a slight reduction in the through-thickness direction.

- The most dramatic difference between the through-thickness and rolling direction coupons was in the percent reduction of area measurements. The through-thickness coupons showed much lower reduction of area values, and much higher variability in the measurements. The percent reduction of area in the through-thickness direction was, on average, one-third to one-half the value in the rolling direction. The coefficient of variation of the reduction of area measurements in the through-thickness direction was in excess of 50 percent, compared to only 4 percent in the rolling direction. Thus, there appears to be enormous variability in through-thickness ductility.

The work described herein was intended to represent a small pilot study on through-thickness tensile testing of the flanges of rolled W shapes. The data sample collected in this study is too small to draw general conclusions on through-thickness test methods, or on through-thickness properties. Nonetheless, the results of this study have provided some insight into these issues. Significant additional through-thickness testing is needed, however, before broader conclusions can be drawn.

Finally, no attempt was made in this study to evaluate the significance of through-thickness properties on the performance of welded moment connections. The significantly reduced ductility measured in the through-thickness directions may adversely affect connection performance by inhibiting redistribution of stress concentrations at the face of the column, or by leading to lamellar tearing. Once sufficient research has been conducted to adequately characterize through-

thickness properties, properly evaluating the structural importance of these properties will provide additional research challenges.

APPENDIX A

ASTM A770

REFERENCE

1. "Commentary on High Restrained Welded Connections," published in *Engineering Journal*, American Institute of Steel Construction, Third Quarter, 1973, pp. 61-73

2. "Interim Guidelines: Evaluation, Repair, Modification, and Design of Steel Moment Frames," Report No. SAC-95-02, Published by the SAC Joint Venture, 1995.

3. Engelhardt, M.D. and Sabol, T.A., " Testing of Welded Steel Moment Connections in Response to the Northridge Earthquake," published in *Northridge Steel Update I*, American Institute of Steel Construction, October 1994.

4. kaufmann, E.J. and Fisher, J.W., "Fracture Analysis of Failed Moment Frame Joints Produced in Full-Scale Laboratory Tests and Buildings damaged in the Northridge Earthquake, Report to the SAC Joint Venture, Lehigh University, 1995.

5. "Evaluation of Two Moment Resisting Frame Connectors Utilizing a Cover-Plate Design," "British Steel Report No. SL/EM/R/S1198/18/95/D,1995.

6. Holt, J.M., " Effect of Specimen Type on Reduction-of-Area Measurements," *Through-Thickness Tension Testing of Steel, ASTM STP 794*, R.J. Goldowski, Ed., American Society for Testing and Materials, 1983, pp. 5-24

7. Reed, D.N., Smith, R.P., Strattan, J.K., and Swift, R.A., " A Comparison of Short Transverse Tension Test Methods," *Through-Thickness Tension Testing of Steel, ASTM STP 794*, R.J. Goldowski, Ed., American Society for Testing and Materials, 1983, pp. 25-39.

8. Ludwigson, D. C., "Factors Affecting Variability in Through-Thickness Reduction-of-Area Measurements," *Through-Thickness Tension Testing of Steel, ASTM STP 794*, R.J. Goldowski, Ed., American Society for Testing and Materials, 1983, pp. 40-47.

9. Ludwigson, D. C., " Plate Thickness and Specimen Size Consideration in Through-Thickness Tension Testing," *Through-Thickness Tension Testing of Steel, ASTM STP 794*, R.J. Goldowski, Ed., American Society for Testing and Materials, 1983, pp. 48-58.

10. Domis, W. F., " Stud Welding of Prolongations to Plate for Through-Thickness Tension Test Specimens," *Through-Thickness Tension Testing of Steel, ASTM STP 794*, R.J. Goldowski, Ed., American Society for Testing and Materials, 1983, pp. 48-58.

11. Jesseman, R. J. and Murphy, G. J., " Some Effect of Specimen Design, Sample Location, and Material Strength on Through-Thickness Tensile Properties," *Through-Thickness Tension Testing of Steel, ASTM STP 794*, R.J. Goldowski, Ed., American Society for Testing and Materials, 1983, pp. 87-112.

12. Ludwigson, D. C., " Relation of Through-Thickness Ductility to Inclusion Prevalence, Matrix Toughness, and Matrix Strength," *Through-Thickness Tension Testing of Steel, ASTM STP 794*, R.J. Goldowski, Ed., American Society for Testing and Materials, 1983, pp. 113-120.

13. Patricia Han., "Overview of Tensile Testing," published in *Tensile Testing*, ASM International, 1992, pp. 1-24